INDC(JPN) - 183/U

NOT FOR PUBLICATION

PROGRESS REPORT

(January 1998 to December 1998 inclusive)

March 1999

Editor

J. Katakura

Japanese Nuclear Data Committee

Japan Atomic Energy Research Institute
Tokai Research Establishment
Tokai-mura, Naka-gun, Ibaraki-ken, Japan

Editor's Note

This is a collection of reports which have been submitted to the Japanese Nuclear Data Committee at the committee's request. The request was addressed to the following individuals who might represent or be touch with groups doing researches related to the nuclear data of interest to the development of the nuclear energy programs.

Although the editor tried not to miss any appropriate addressed, there may have been some oversight. Meanwhile, contribution of a report rested with discretion of its author. The coverage of this document, therefore, may not be uniform over the related field or research.

In this progress report, each individual report is generally reproduced as it was received by the JNDC secretariat, and editor also let pass some simple obvious errors in the manuscripts if any.

This edition covers a period of January 1, 1998 to December 31, 1998. The information herein contained is of a nature of "Private Communication." Data contained in this report should not be quoted without the author's permission.

Table of Contents

A. Nuclear Data Center and Working Groups of Japanese Nuclear Data Committee

ELEMENT S	A	QUANTITY	ENERGY MIN	MAX	LAB	TYPE	DOCUMENTATION REF VOL PAGE	DATE	COMMENTS
H	2	(N,GAMMA)	1.0+4	8.0+4	TIT	EXPT-PROG	INDC(JPN)-183U	MAR 99	NAGAI+.P92. 2.12,2.04MUB AT 31,54KEV
LI	6	DIFF ELASTIC	1.2+7	1.8+7	JAE	EXPT-PROG	INDC(JPN)-183U	MAR 99	CHIBA+.P26.OPT MODEL
LI	6	DIFF INELAST	1.2+7	1.8+7	JAE	EXPT-PROG	INDC(JPN)-183U	MAR 99	CHIBA+.P26.DWBA 3-BODY FINAL ST MDL
LI	6	N EMISSION	1.2+7	1.8+7	TOH	EXPT-PROG	INDC(JPN)-183U	MAR 99	IBARAKI+.P73.DA/DE,DA.TOF
LI	7	N EMISSION	1.2+7	1.8+7	TOH	EXPT-PROG	INDC(JPN)-183U	MAR 99	IBARAKI+.P73.DA/DE,DA.TOF
BE	9	N EMISSION	1.2+7	1.8+7	TOH	EXPT-PROG	INDC(JPN)-183U	MAR 99	IBARAKI+.P73.DA/DE,DA.TOF
C	12	DIFF INELAST	NDG		JAE	THEO-PROG	INDC(JPN)-183U	MAR 99	SUKHOVITSKIJ+.P25.SOFT-ROTATOR MODEL
C	12	(N,GAMMA)	5.5+5		TIT	EXPT-PROG	INDC(JPN)-183U	MAR 99	KIKUCHI+.P91.PARTIAL SIG,4 LVLS,GVN
C	12	(N,GAMMA)		1.0+6	TIT	THEO-PROG	INDC(JPN)-183U	MAR 99	KITAZAWA+.P91.DIRECT CAPTURE ANAL
C	12	P EMISSION	6.5+7	7.5+7	TOH	EXPT-PROG	INDC(JPN)-183U	MAR 99	NAUCHI+.P74.DA/DE.12-70 DEG
C	12	D EMISSION	6.5+7	7.5+7	TOH	EXPT-PROG	INDC(JPN)-183U	MAR 99	NAUCHI+.P74.DA/DE.12-70 DEG
O	16	(N,ALPHA)	1.4+7		TOH	EXPT-PROG	INDC(JPN)-183U	MAR 99	SANAMI+.P76.SIG.GRIDDED IC
AL	27	P EMISSION	1.4+7		OSA	EXPT-PROG	INDC(JPN)-183U	MAR 99	TAKAHASHI+.P63.DA/DE,DE,SIG.TBL
AL	27	P EMISSION	6.5+7	7.5+7	TOH	EXPT-PROG	INDC(JPN)-183U	MAR 99	NAUCHI+.P74.DA/DE.12-70 DEG
AL	27	D EMISSION	6.5+7	7.5+7	TOH	EXPT-PROG	INDC(JPN)-183U	MAR 99	NAUCHI+.P74.DA/DE.12-70 DEG
AL	27	A EMISSION	1.4+7		OSA	EXPT-PROG	INDC(JPN)-183U	MAR 99	TAKAHASHI+.P63.DA/DE,DE,SIG.FIG,TBL
TI		P EMISSION	1.4+7		OSA	EXPT-PROG	INDC(JPN)-183U	MAR 99	TAKAHASHI+.P63.DA/DE,DE,SIG.TBL
TI		A EMISSION	1.4+7		OSA	EXPT-PROG	INDC(JPN)-183U	MAR 99	TAKAHASHI+.P63.DA/DE,DE,SIG.TBL
V	51	NONELA GAMMA	1.4+7		OSA	EXPT-PROG	INDC(JPN)-183U	MAR 99	MURATA+.P66.TOF.HP-GE DETECTOR
NI		(N,ALPHA)	4.2+6	6.5+6	TOH	EXPT-PROG	INDC(JPN)-183U	MAR 99	SANAMI+.P73.DA/DE,DA,SIG.GRIDDED IC

ELEMENT S	A	QUANTITY	ENERGY MIN	MAX	LAB	TYPE	DOCUMENTATION REF VOL PAGE	DATE	COMMENTS
NI	58	(N,ALPHA)	4.2+6	6.5+6	TOH	EXPT-PROG	INDC(JPN)-183U	MAR 99	SANAMI+.P73.DA/DE,DA,SIG.GRIDDED IC
SE	80	(N,GAMMA)	2.5-2		PNC	EXPT-PROG	INDC(JPN)-183U	MAR 99	NAKAMURA+.P36.ACTIVATION METHOD
SE	80	RES INT CAP	5.0-1		PNC	EXPT-PROG	INDC(JPN)-183U	MAR 99	NAKAMURA+.P36.ACTIVATION METHOD
ZR	94	(N,GAMMA)	2.5-2		PNC	EXPT-PROG	INDC(JPN)-183U	MAR 99	NAKAMURA+.P36.ACTIVATION METHOD
ZR	94	RES INT CAP	5.0-1		PNC	EXPT-PROG	INDC(JPN)-183U	MAR 99	NAKAMURA+.P36.ACTIVATION METHOD
MO	100	DIFF INELAST	NDG		KYU	EVAL-PROG	INDC(JPN)-183U	MAR 99	KAWANO+.P49.DWBA AND H-F-M MDL CALC
MO	92	DIFF INELAST	NDG		KYU	EVAL-PROG	INDC(JPN)-183U	MAR 99	KAWANO+.P49.DWBA AND H-F-M MDL CALC
MO	98	DIFF INELAST	NDG		KYU	EVAL-PROG	INDC(JPN)-183U	MAR 99	KAWANO+.P49.DWBA AND H-F-M MDL CALC
SN		A EMISSION	1.5+7		KYU	EXPT-PROG	INDC(JPN)-183U	MAR 99	TAKAO+.P45.HELIUM ACCUMULATION METH
SN	124	(N,GAMMA)	2.5-2		PNC	EXPT-PROG	INDC(JPN)-183U	MAR 99	NAKAMURA+.P36.ACTIVATION METHOD
SN	124	RES INT CAP	5.0-1		PNC	EXPT-PROG	INDC(JPN)-183U	MAR 99	NAKAMURA+.P36.ACTIVATION METHOD
I	127	(N,GAMMA)	2.5-2		PNC	EXPT-PROG	INDC(JPN)-183U	MAR 99	NAKAMURA+.P36.ACTIVATION METHOD
I	127	RES INT CAP	5.0-1		PNC	EXPT-PROG	INDC(JPN)-183U	MAR 99	NAKAMURA+.P36.ACTIVATION METHOD
CS	133	(N,GAMMA)	2.5-2		PNC	EXPT-PROG	INDC(JPN)-183U	MAR 99	NAKAMURA+.P36.ACTIVATION METHOD
CS	133	RES INT CAP	5.0-1		PNC	EXPT-PROG	INDC(JPN)-183U	MAR 99	NAKAMURA+.P36.ACTIVATION METHOD
CS	134	(N,GAMMA)	PILE		PNC	EXPT-PROG	INDC(JPN)-183U	MAR 99	KATOH+.P29.SIG=140.6+-8.5 B
DY		(N,GAMMA)	3.0-3	5.0+4	KTO	EXPT-PROG	INDC(JPN)-183U	MAR 99	CHO+.P40.TOF,BGO SCINTILLATORS
HF		(N,GAMMA)	3.0-3	5.0+4	KTO	EXPT-PROG	INDC(JPN)-183U	MAR 99	CHO+.P40.TOF,BGO SCINTILLATORS
PB		A EMISSION	1.5+7		KYU	EXPT-PROG	INDC(JPN)-183U	MAR 99	TAKAO+.P45.HELIUM ACCUMULATION METH
PA	231	FISSION	1.0-1	1.0+4	KTO	EXPT-PROG	INDC(JPN)-183U	MAR 99	KOBAYASHI+.P39.PB-SLOWING-DOWN SPECT

ELEMENT S	A	QUANTITY	ENERGY MIN	ENERGY MAX	LAB	TYPE	DOCUMENTATION REF VOL PAGE	DATE	COMMENTS
U	233	FRAG NEUTS	2.5-2		KTO	EXPT-PROG	INDC(JPN)-183U	MAR 99	NISHIO+.P42.FUNCT OF FRAG MASS + TKE
U	238	EVALUATION	NDG		JAE	EVAL-PROG	INDC(JPN)-183U	MAR 99	MASLOV+.P19.H-F-M,CC,2-HUMP FIS MDL
U	238	PHOTO-FISSN	1.5+7	6.0+7	OSA	EXPT-PROG	INDC(JPN)-183U	MAR 99	TAKAHASHI+.P67.CHARGE AND MASS DISTS
AM	242	FISSION	3.0-3	3.0+1	KTO	EXPT-PROG	INDC(JPN)-183U	MAR 99	KAI+.P41.AM242M.TOF.REL TO U235NF
MANY		(N,P)	1.3+7	1.5+7	NAG	EXPT-PROG	INDC(JPN)-183U	MAR 99	KASUGAI+.P54.28 ACT SIGS (F TO SN)
MANY		(N,ALPHA)	1.3+7	1.5+7	NAG	EXPT-PROG	INDC(JPN)-183U	MAR 99	KASUGAI+.P56.12 ACT SIGS (MG TO CD)
MANY		(N,ALPHA)	1.3+7	1.5+7	NAG	EVAL-PROG	INDC(JPN)-183U	MAR 99	KASUGAI+.P55.SYSTEMATICS,A=19-188
MANY		FISSION	NDG		JAE	EVAL-PROG	INDC(JPN)-183U	MAR 99	FUKAHORI+.P22.SYST FIS-SIG IN HIGH E
MANY		FISS PROD BS	NDG		JAE	EVAL-PROG	INDC(JPN)-183U	MAR 99	KATAKURA+.P23.MODEL CALC FOR ENDF/B6
MANY		LVL DENSITY	/		JAE	EVAL-PROG	INDC(JPN)-183U	MAR 99	MASLOV+.P19.TH-CF.CONST TEMP MODEL

I. Electrotechnical Laboratory

A. Quantum Radiation Division

I-A-1

Development of Intermediate Neutron Fluence Standards by Using $^{45}Sc(p,n)^{45}Ti$ Reaction, Iron Filtered Beam and $^{124}Sb(\gamma)$-Be Source

N. Takeda[1], K.Kudo[1], K. Kobayashi[2], S. Yoshimoto[2], M. Fujishiro[3] and K. Okamoto[2]

For neutron radiation dosimetry in many working environments around nuclear reactors, a significant fraction of the neutron equivalent dose is due to neutrons within the energy range from thermal to 25 keV. Because of the difficulty of producing suitable monoenergetic neutron sources, instruments are rarely calibrated in this energy range and biological data are sparse. Therefore, the reference field of intermediate neutrons are required for the calibration of neutron detectors and survey meters and for the biological irradiation. We have been developing intermediate neutron fluence standards by using different kind of sources of $^{45}Sc(p,n)^{45}Ti$ reaction, iron filtered beam and $^{124}Sb(\gamma)$-Be radioisotope(1). It is important that these sources have a low background contamination from other energy neutrons and gamma rays.

The Fe-filtered neutron facility at the KUR (Kyoto University Research Reactor of 5MW reactor power) provides a quasi-monoenergetic neutron beam at the peak energy of 24 keV for experimental studies of biological radiation effects(2). Figure 1 shows the schematic arrangement of the Fe-filtered neutron facility. The total thickness of iron disks equipped in the Fe-filtered beam facility was 45 cm together with aluminum layers of 35 cm thickness one after the other, a sulfur filter of 16 g/cm^2 thickness for suppressing higher energy neutrons and a boron filter of 1.26 g/cm^2 thickness for reducing lower energy neutrons, respectively. We have been measuring the neutron flux at 75 cm from the exit of a reentrant hole by using a ^{3}He gas or a hydrogen gas proportional counter. The filters of both a 15cm^L shadow cone (composed of a homogeneous mixture of polyethylene with 10% lithium fluoride) and a 2 cm^L Ti disc were used to subtract a background neutrons at other energies contaminated in the irradiation field, separately.

Many experiments have been performed under several different conditions of detectors, filters and reactor powers. As one of the examples, the pulse height spectrum measured by the ^{3}He gas proportional counter was shown in Fig. 2 at the reactor power of 100 kW. A response function (the solid curve) at 24 keV calculated by the NRESPG Monte Carlo code(3) was fitted to the experimental data (the dotted curve) as shown in the figure. The neutron fluence at 24 keV was determined as 2.7×10^3 (n/cm^2/s) in this case.

Furthermore, the peak yield at 24 keV compared with the background neutron yield was investigated by adding iron blocks of 75 cm thickness at the exit part of reentrant hole. The MCNP-4 Monte Carlo code was used to estimate the peak intensity at 24 keV compared with background neutrons at the measuring point, assuming a three dimensional assembly which included the layout in Fig.1 with concrete blocks outside the measuring space. The calculation was performed under the initial neutron source produced at the fixed point A at another edge of the reentrant hole near the reactor core. The energy distribution was

---

[1] Quantum Radiation Division, Electrotechnical Laboratory

[2] Research Reactor Institute, Kyoto University

[3] Research Institute for Advanced Science and Technology, Osaka Prefecture University

provided by other studies(4) and the angular distribution of neutrons emitted from the source was assumed to be either parallel to the reentrant hole or to have a cosine distribution. The neutron intensity (in the unit of percent) was shown in Fig. 3 in both the cases with additional iron blocks (total iron thickness of 120 cm) and without it, respectively. The ratio of peak intensity at 24 keV to the other energy neutrons was improved clearly from 15 % to 80 % with increasing iron filter thickness, however the intensity decreased down to about 2 %. The optimum irradiation condition should be selected for each application.

The problem which we are now confronted in the irradiation field using $^{45}Sc(p,n)^{45}Ti$ is the background neutrons originated from other reactions of Li(p,n)Be and T(p,n)He occurred at the inside of the beam line. We are now replacing the whole beam line to new one and planning to install another beam line to avoid the contamination.

References

(1) N. Takeda, K. Kudo, T. Sugita, M. Fujishiro and K. Okamoto, Proc. of the Scientific Meeting of the Research Reactor Institute, Kyoto University (1996) 67.
(2) H. Utsumi, K. Kobayashi et. al., Proc. of the Scientific Meeting of the Research Reactor Institute, Kyoto University (1996) 311.
(3) N. Takeda, K. Kudo, (in press) Nucl. Instr. and Meth. (1999) .
(4) private communications

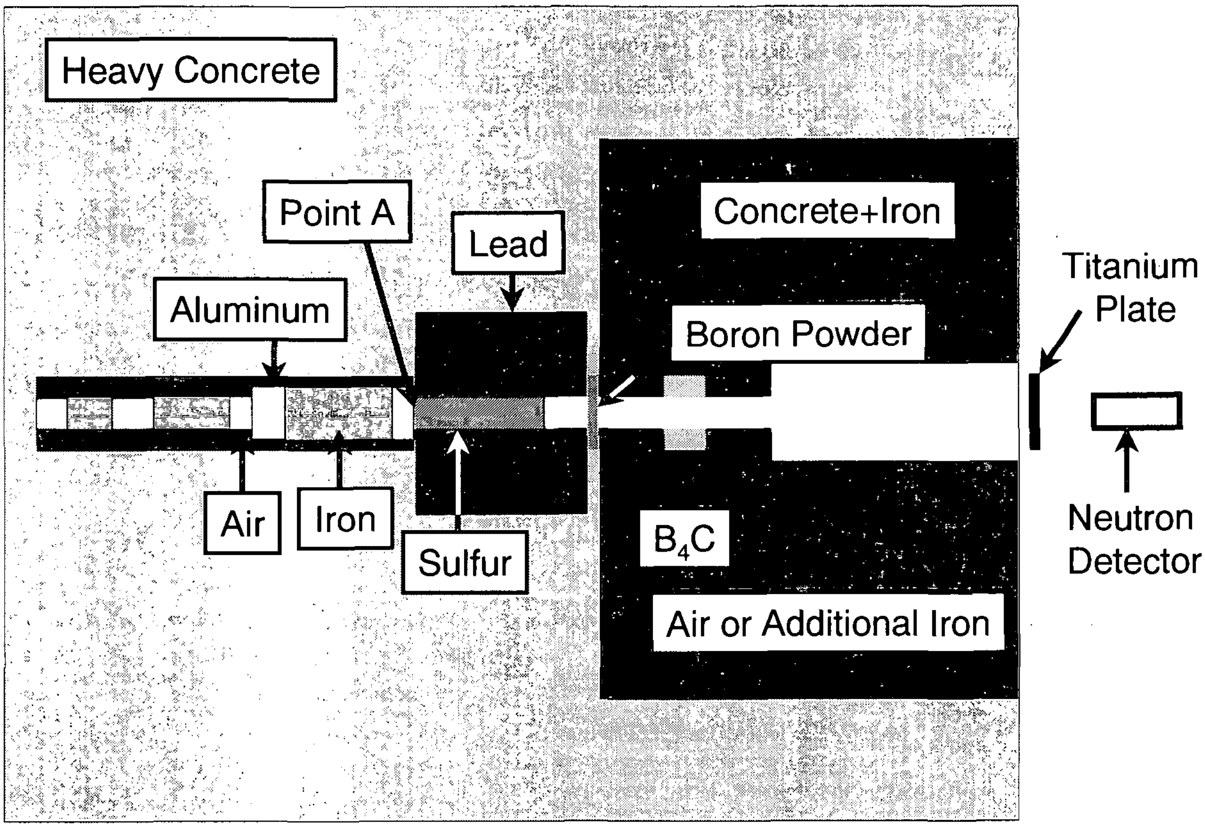

Figure 1. Schematic arrangement of the Fe-filtered neutron facility.

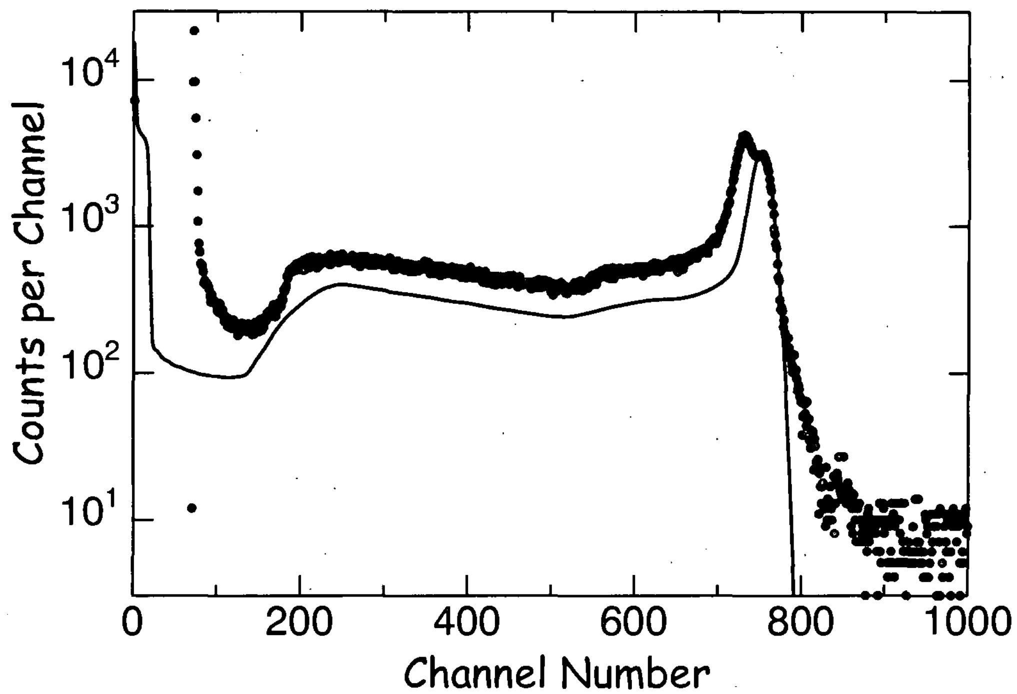

Figure 2. An example of the pulse height spectrum measured by the ^{3}He gas proportional counter.

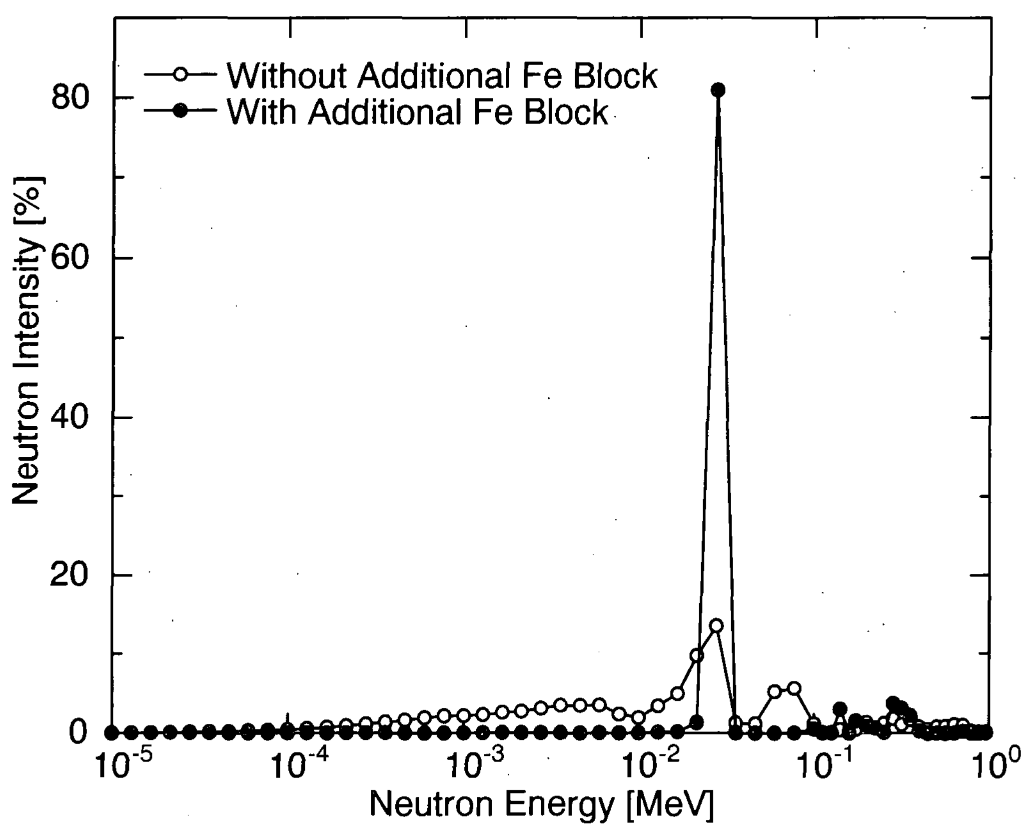

Figure 3. Neutron intensity of the Fe-filtered neutron facility calculated by MCNP4 code.

I-A-2

OBSERVATION OF M1 RESONANCE IN ^{206}Pb USING A HIGHLY LINEAR POLARIZED PHOTON BEAM

H. Ohgaki, H. Toyokawa, T. Noguchi, S. Sugiyama, T. Mikado, K. Yamada, R. Suzuki, T. Ohdaira, N. Sei, and T. Yamazaki*

A paper on this subject was presented in the TOPICAL CONFERENCE ON GIANT RESONANCES, May 11-16, 1998, Varenna, Italy, with following abstract.

Compton scattering between a relativistic electron beam and a laser beam enhances laser photon energy in a head-on collision, called laser-Compton photons (LCPs). A LCP beam is a quasi-monochromatic gamma-ray whose energy is tunable. The LCP is mainly noted for high polarization caused by the small spin-flip amplitude in Compton scattering in a head-on collision. A linear polarized laser beam generated by a Q-switched Nd:YLF laser (λ = 527 nm) enters the vacuum window and collides head on with the electron beam at the straight section of the storage ring TERAS. The laser beam is focused on the collision point in a 2-mm-diameter. To obtain an end-point energy of 8.1 MeV, TERAS was operated at 475 MeV. The LCP beam energy spread was 21.6%, defined by the 5-mm-diameter lead collimator along the LCP beam axis. The laser-electron collision point and the collimator were 5 m apart. The polarization axis of the linear polarized LCP beam (polarization: 95.3%) was changed at 100 second intervals to eliminate systematic asymmetry in measurement. The LCP beam intensity, monitored by a 5-mm-thick plastic scintillation detector, was $\{\sim 10^5\}$ photons/s at the scattering target.
An enriched (99.3%) ^{206}Pb target of 4.0 g was 7 mm in diameter and 15 mm long. A pure Ge detector (120% relative detection efficiency) was used to measure photons scattered at angles of 90° and 127°. The Ge detector energy resolution was 9 keV full width at half maximum (FWHM) at 7.5 MeV. To reduce pile up from Compton scattering photons from the target, a 4-mm-thick lead hardener was placed between the target and the Ge detector. A 50-mm-thick lead collimator defining the detector solid angle of 0.85 sr with its entrance window of 40x20 mm^2 was placed in front of the Ge detector, which was shielded by lead 20 cm thick. Background was subtracted by spectrum stripping method. The detector response function was calculated with Monte Carlo code EGS4. NRF from ^{12}C, 15.1 MeV 1^+ state, was used to calibrate analyzing power. The experimental system yielded an analyzing power of 89.0%. Figure 1 shows energy spectra of $^{206}Pb(\gamma_{pol},\gamma)$ measured at a 90° scattering angle. Parity information is obtained from asymmetry. Parity assignment is thus straightforward, using the LCP beam, in our case, the top spectrum in Fig. 1 corresponds to M1 or E2 transition events. The bottom spectrum corresponds to E1 transition events. Several known E1 levels are clearly visible in the bottom spectrum and many peaks in the top spectrum. M1 and E2 transition are separated with an angular distribution. Intensity ratio W(90°)/W(127°) is 0.734 for pure dipole (M1 or E1) and 2.28 for pure quadrupole (E2) transitions. We use the decomposition to calculate M1 distribution. A 40-keV energy bin was made to check the present experiment and analysis. We use several known levels to normalize the transition width and the transition probability with the reference[1] and $\Gamma_0/\Gamma = 1$ was assumed. Thus, error in the calculation includes statistical and normalization error, estimated to be 26%. The result is plotted in Fig. 2 as solid circles. Our data agrees reasonably well with both tagged photon data (histogram bars)[2] and electron scattering data (Xs)[3]. Two humps, at 7.2 and 7.9 MeV, appear clearly in the measured M1 strength distribution. The isovector M1 transition probability distribution in ^{206}Pb was predicted using a microscopic calculation (solid line, Fig. 2)[4]. The two humps in the M1 strength distribution are reproduced

well by the quasi-particle model(QPM), which includes two-phonon states. Our total M1 transition probability from 6.5 to 8.2 MeV was 17.4 ± 5.6 μ_N^2, consistent with the strength of $\Sigma B(M1\uparrow)=16.1\ \mu_N^2$ predicted by QPM calculation. Our result also agrees with that from a tagged photon experiment, $\Sigma B(M1\uparrow)=19 \pm 2\ \mu_N^2$ for corresponding energy bins.

To obtain more details on M1 resonance distribution, a spin-parity assignment was done for 98 individual peaks observed in high-resolution data (Fig. 1) from 6.5 to 8.2 MeV, 21 M1 transitions were identified based on asymmetry and the intensity ratio. Individual M1 levels are plotted in Fig. 2 as open circles. These significant M1 levels clearly concentrate around 7.2 MeV and form the low-energy hump. A few M1 levels form the high-energy hump. This corresponds to the result from the 40-keV bin that the low-energy bump is larger than the high-energy one. Total M1 transition probability summed from these significant M1 levels is $\Sigma B(M1\uparrow)=6.1 \pm 2\ \mu_N^2$, which exhausts 35% of the total M1 strength given by the 40-keV bin. Compared to the M1 states in ^{208}Pb[5], heavy fragmentation is observed in ^{206}Pb. This heavy fragmentation was anticipated from the high-level density of ^{206}Pb. The degree of M1 damping, however, is almost the same in both nuclei.

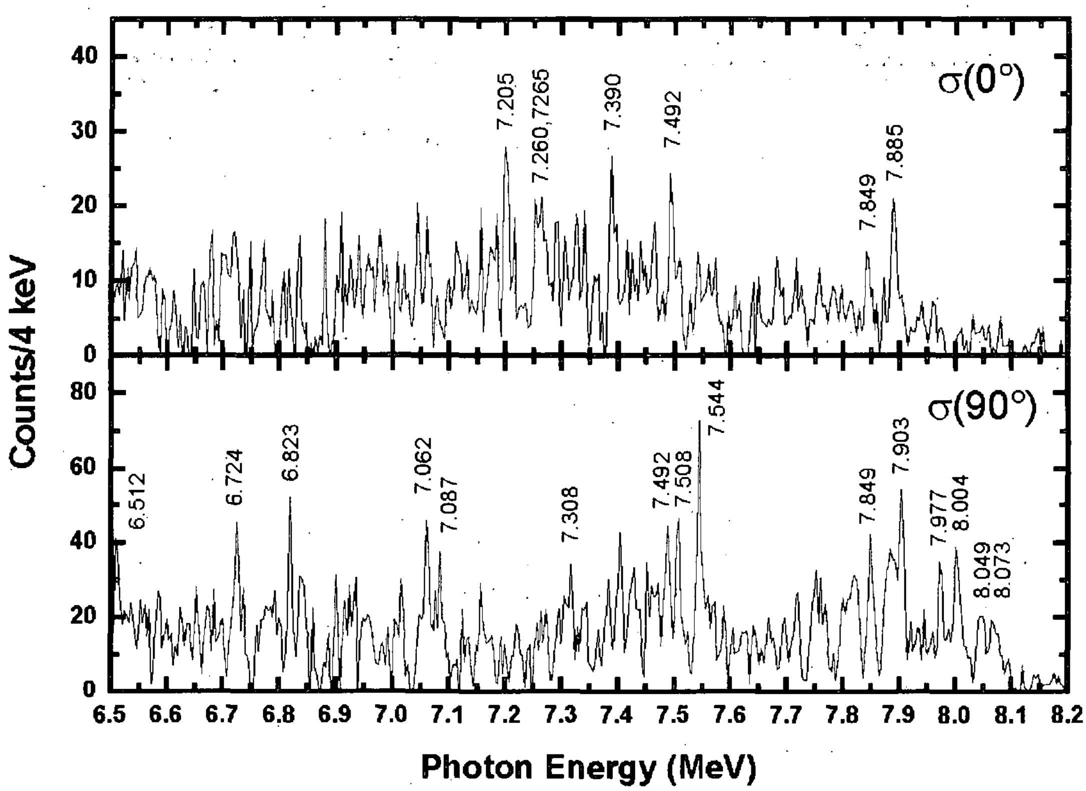

Fig.1 Above: $^{206}Pb(\gamma_{pol},\gamma)$ energy spectrum at a 90° scattering angles against a parallel-polarized plane. Below: That against a perpendicularly polarized plane.

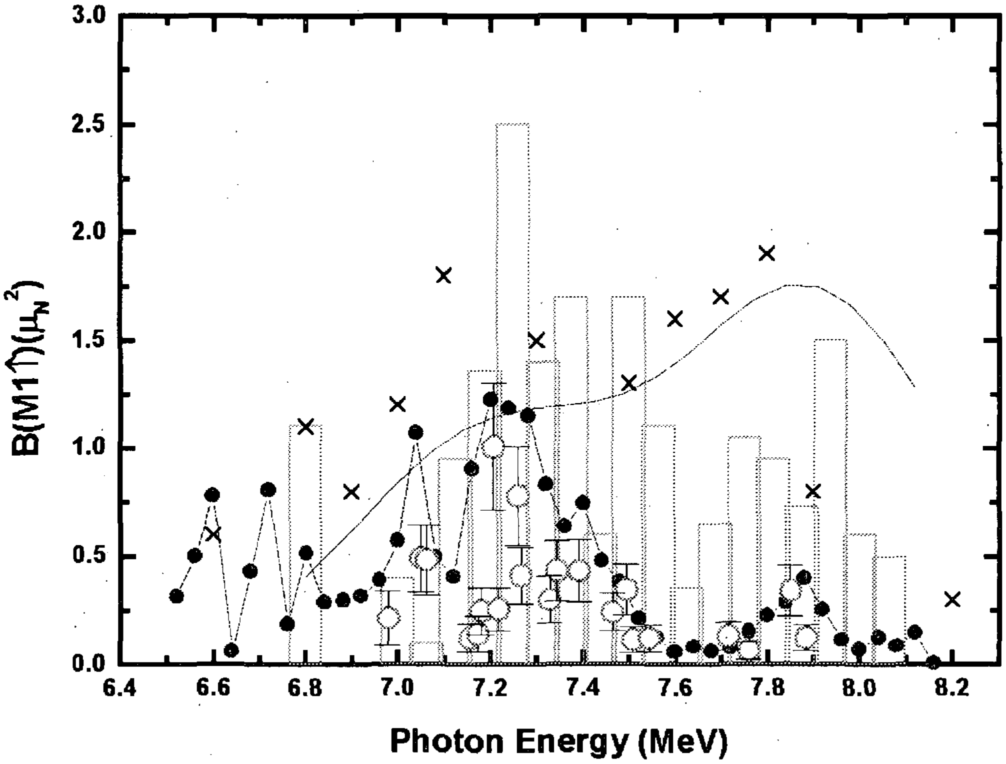

Fig.2 ^{206}Pb distribution of M1 transition probability. Solid circles: results with 40 keV-energy bin; open circles: high resolution data; histogram bars: tagged photon data[3]; Xs: electron scattering data[2]; solid line: QPM calculation given by Ponomarev[4].

References:

1) T. Chapuran, R. Vodhanel, and M.K. Brussel, Phys. Rev. C22 (1980) 1420.
2) R.M. Laszewski et al., Phys. Rev. Lett. 54 (1985) 530.
3) M. Schanz, A. Richter, and E. Lipparini, Phys. Rev. C36 (1987) 555.
4) V. Ponomarev, A. Vdovin, and Ch. Velchev, J.Phys. G 13 (1987) 1523.
5) R.M. Laszewski et al., Phys. Rev. Lett. 61 (1988) 1710.
6) H.Ohgaki et al., Proc. of the NSRT (1997) 74.

* present address:Institute of Advanced Energy, Kyoto University

I-A-3 Photoneutron Production with the Laser-Compton Backscattered Photons

Hiroyuki TOYOKAWA, Hideaki OHGAKI, Suguru SUGIYAMA, Tomohisa MIKADO, Kawakatsu YAMADA, Ryoichi SUZUKI, Toshiyuki OHDAIRA, and Norihiro SEI

A paper on this abstract will be published in Proc. 1998 Nuclear Data Symposium with the following abstract.

Monoenergetic neutrons with the energies from higher than thermal region to lower than about a few tens of keV are extremely useful for a detector calibration purpose, because there are few neutron sources with these energies. Quasi-monoenergetic neutrons with energies lower than about 40 keV are generated with a photo-induced neutron emission process of a ^{9}Be target using photons with the energies around the threshold energy for the ^{9}Be(γ,n) reaction. We used the Laser-Compton-backscattered (LCS) photon facility of Electrotechnical Laboratory (ETL) to generate the pulsed photon beams with the energies continuously tunable around 1600 – 1700 keV. The intensity is about 10^{7} cm^{-2} s^{-1}. Five LCS photon sources with the cutt-off energies of 1651.0 keV, 1664.8 keV, 1667.5 keV, 1679.4 keV, and 1709.0 keV were used. Four of the five of them exceeded the threshold energy for the ^{9}Be(γ,n) reaction. Figure 1 shows the energy spectrum of the LCS photons, measured with a HPGe detector. The neutron yields were measured by counting intense gamma-ray flashes caused by the Gd(n,γ)Gd reaction. Figure 2 shows the time profiles of the gamma-ray flashes, which were measured below (1651 keV) and above (1709 keV) the threshold energy for the ^{9}Be(γ,n) reaction. The prompt photon emission, that is seen as a sharp spike found in the right-hand small figure, is due to the annihilation gamma-rays or the Compton-scattered photons from the target, and, hence, it indicates the incident time of the LCS photons. The delayed bump, peaked at about 8 μsec after the incidence of the LCS photons are due to the neutrons from

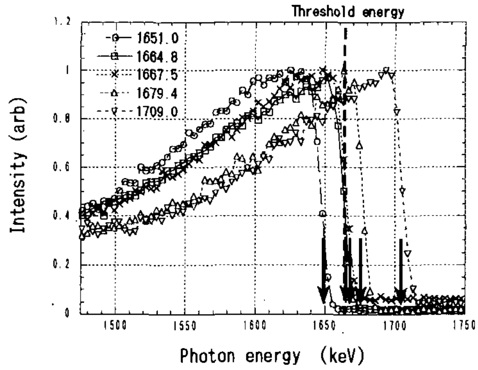

Fig. 1 Energy spectra of the LCS photons. The arrows indicate the cut-off energy of the photons.

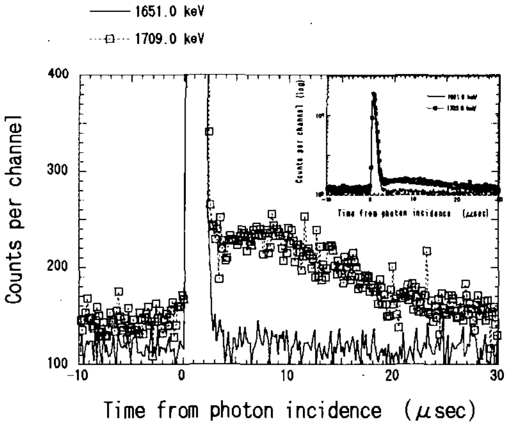

Fig. 2 Time profile of the scintillation outputs from the neutron detector. The bump at 1709 keV is due to the Gd(n,γ)Gd reactions.

the ^{9}Be, and only seen in the time profile taken above the threshold energy. The ratio of the accumulated counts within 3 – 30 μsec, to the number of the incident photons were 1.15, 4.62, 4.72, 23.5, and 56.4×10^{-6}, respectively.

II. Hokkaido University

A. Division of Physics

II-A-1 Development of Charged Particle Nuclear Reaction Data Retrieval System on IntelligentPad

Yosihide OHBAYASI [a], Hiroshi MASUI [a],
Shigeyoshi AOYAMA [b], Kiyoshi KATÔ [c] and Masaki CHIBA [d]

We develop the retrieval system of Nuclear Reaction Data File (NRDF) compilation[1] using IntelligentPad architecture. IntelligentPad is a kind of object-oriented "graphical user interface (GUI) based" system construction environment[2]. A "pad" can be treated as an object of the graphical user interface on the computer, like a view of "real paper pad". On the "pad" environment, programming of any tools on GUI can be done by 'intuitively' cut and paste action of pad.

Figure 1 shows the basic design of this system. Using a database management system (DBMS) based on SQL, we construct the NRDF data management server on the UNIX WS. (SUN Ultra1). UniSQL is adopted as a DBMS at the present. The network communications between the NRDF server and clients are achieved by CGI. Data retrieval "client" is constructed with IntelligentPad architecture. We construct the Windows95, 98/NT-based IntelligentPad. Figure 2 shows a hardcopy of an experimental product of the NRDF data retrieval system.

We will distribute the system to researchers for test use and blush-up the experimental system. Including EXFOR data in this system is underway. Furthermore, we will proceed to develop the system to embody the "effective" use of nuclear reaction data.

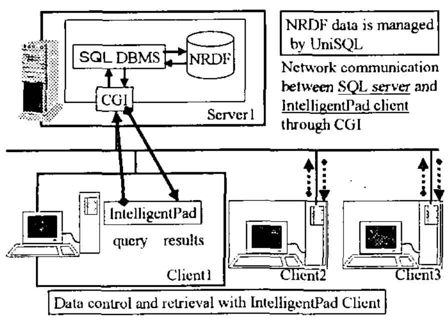

Fig.1 Network-based system.

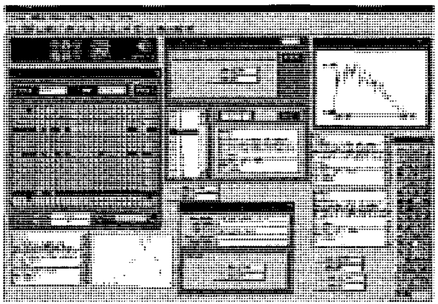

Fig.2 Overview of the system.

References

[1] Katô, K.: Genshikaku Kenkyu, **39**, 63 (1995, in Japanese).

[2] Tanaka, Y.: International Conference on Multimedia Modeling '98, Lausanne, p.1 (1998).

---

[a] Meme Media Laboratory, Hokkaido University, Sapporo, Hokkaido 060-8628
[b] Information Processing Center, Kitami Institute of Technology, Kitami, Hokkaido 090-8507
[c] Division of Physics, Graduate School of Science, Hokkaido University, Sapporo, Hokkaido 060-0810
[d] Division of Social Information, Sapporo Gakuin University, Ebetsu, Hokkaido 069-8555

III. Japan Atomic Energy Research Institute

A. Nuclear Data Center and Working Groups of Japanese Nuclear Data Committee

III-A-1 Evaluation of Covariance Data for Chromium, Iron and Nickel Contained in JENDL-3.2

S.Y. Oh* and K. Shibata

A paper on this subject was published in J. Nucl. Sci. Technol., **35**, 66 (1998) with the following abstract:

An evaluation has been made for the covariances of neutron cross sections of ^{52}Cr, ^{56}Fe, ^{58}Ni and ^{60}Ni contained in JENDL-3.2. Reactions considered were the threshold reactions such as (n,2n), (n,nα), (n,np), (n,p), (n,d), (n,t) and (n,α), the radiative capture reaction above the resonance region, and the inelastic scattering to discrete and continuum levels. Evaluation guidelines and procedures were established during the work.

A generalized least-squares fitting code GMA was used in estimating covariances for reactions of which JENDL-3.2 cross sections had been evaluated by taking account of many measured data. For cross sections that had been evaluated by nuclear reaction model calculations, the KALMAN code, which yields covariances of cross sections and of associated model parameters on the basis of the Bayesian statistics, was used in conjunction with reaction model codes EGNASH and CASTHY.

The evaluated uncertainties of a few percent to 30 percent in the cross sections look reasonable, and the correlation matrices show understandable trends. Even though there is no strict way to confirm the validity of the evaluated covariances, tools and procedures adopted in the present work are appropriate for producing covariance files based on JENDL-3.2. The covariances obtained will be compiled into JENDL in the near future. Meanwhile, new sets of optical model and level density parameters were proposed as one of byproducts obtained from the KALMAN calculations.

* Korea Atomic Energy Research Institute

III-A-2

Estimation of Covariances of ^{10}B, ^{11}B, ^{55}Mn, ^{240}Pu and ^{241}Pu Neutron Nuclear Data in JENDL-3.2

K. Shibata, Y. Nakajima* and T. Murata**

A paper on this subject was published in JAERI-Research 98-045 (1998) with the following abstract:

Covariances of nuclear data have been estimated for 5 nuclides contained in JENDL-3.2. The nuclides considered are ^{10}B, ^{11}B, ^{55}Mn, ^{240}Pu, and ^{241}Pu, which are regarded as important for the nuclear design study of fast reactors. The physical quantities for which covariances are deduced are cross sections, resolved and unresolved resonance parameters, and the first order Legendre-polynomial coefficient for the angular distribution of elastically scattered neutrons. The covariances were estimated by using the same methodology that had been used in the JENDL-3.2 evaluation in order to keep a consistency between mean values and their covariances. The least-squares fitting code GMA was used in estimating covariances for reactions of which JENDL-3.2 cross sections had been evaluated by taking account of measurements. Covariances of nuclear model calculations were deduced by the KALMAN system. The covariance data obtained were compiled in the ENDF-6 format, and will be put into the JENDL-3.2 Covariance File which is one of JENDL special purpose files.

* Research Organization for Information Science and Technology
** AITEL Corporation

III-A-3

Neutron Data Evaluation of ^{238}U

V.M. Maslov*, Yu.V. Porodzinskij*, A. Hasegawa and K. Shibata

A paper on this subject was published in JAERI-Research 98-040 (1998) with the following abstract:

Cross sections for neutron-induced reactions on ^{238}U are calculated by using the Hauser-Feshbach-Moldauer theory, the coupled channel model and the double-humped fission barrier model. The direct excitation of ground state band levels is calculated with a rigid rotator model. The direct excitation of vibrational octupole and $K=2^+$ quadrupole bands is included using a soft (deformable) rotator model. The competition of inelastic scattering to fission reaction is shown to be sensitive to the target nucleus level density at excitations above the pairing gap. As for fission, (n,2n), (n,3n), and (n,4n) reactions, secondary neutron spectra data are consistently reproduced. Pre-equilibrium emission of first neutron is included. Shell effects in the level densities are shown to be important for estimation of energy dependence of non-emissive fission cross section.

III-A-4

Actinide Level Density Parameter Systematics

V.M. Maslov* and Yu.V. Porodzinskij*

A paper on this subject was published in JAERI-Research 98-038 (1998) with the following abstract:

Neutron resonance spacing data for actinides (Th – Cf) are analyzed to obtain level density parameters. Cumulative plots of low-lying levels are fitted with a constant temperature model. Systematic trends of constant temperature model parameters *Uc*, *Uo*, *T* are revealed.

* Radiation Physics and Chemistry Problems Institute, Belarus

III-A-5 Nuclear Data Evaluation and Compilation for JENDL Intermediate Energy Files

T. Fukahori and Japanese Nuclear Data Committee (High Energy Nuclear Data Evaluation WG)

The JAERI Nuclear Data Center started evaluation work in cooperation with Japanese Nuclear Data Committee (JNDC) to produce files related intermediate energy, which are JENDL High Energy File, JENDL PKA/KERMA File and JENDL Photonuclear Data File. In this report, present status of these files is described.

The JENDL High Energy File includes nuclear data for proton- and neutron-induced reactions. The evaluation work is separated into two phases. The energy range of the phase-I is up to 50 MeV, mainly for the International Fusion Material Irradiation Facility (IFMIF) [1]. The isotopes included in the JENDL High Energy File for IFMIF are summarized in Table 1.2.1. In the first step of the JENDL High Energy File, evaluation work was concentrated to the neutron data below 50 MeV for IFMIF. Test processing for a MCNP library from this file was successfully performed for several nuclei. Tentative benchmark test for iron was carried out with this library. The energy range for the phase-II is up to 3 GeV mainly for a project of JAERI Center for Neutron Science. Specification of evaluation work for Phase-II files was changed with careful discussions considering new data requirements. The elements included in the JENDL High Energy File are summarized in Table 1.2.2 as well as newly decided priorities. Below 20 MeV, the data of JENDL Fusion File[2] or JENDL-3.2[3] are adopted basically.

The JENDL Photonuclear Data File is being developed for gamma-ray induced reaction data up to 140 MeV. The photon absorption cross section is evaluated with the giant dipole resonance model and quasi-deuteron model, and the decaying processes are estimated with the statistical model with preequilibrium correction by using MCPHOTO and ALICE-F codes. The isotopes shown in Table 1.2.3 are included in the file. For ^{181}Ta, re-evaluation has been done by using method developed by Sao Paulo University.[4] Some of evaluated results were compared with the other photonuclear data files evaluated at Los Alamos, Beijing, Moscow and Obninsk.

The JENDL PKA/KERMA File is generated to supply primary knock-on atom (PKA) spectra, damage energy spectra, DPA (displacement per atom) cross sections and kerma factors by neutron-induced reactions in the energy region up to 50 MeV. The elements included in the file are listed in Table 1.2.4. A processing code system, ESPERANT[5] was developed to calculate above quantities from evaluated nuclear data file by using effective single particle emission approximation (ESPEA). The JENDL PKA/KERMA File for the nuclei except light mass nuclei will be produced just after evaluation work for the JENDL High Energy File for IFMIF is finished. For light mass nuclei, SCINFUL/DDX code which considers break-up reactions with PKA spectra is used as well as EXIFON code which can calculate with correction of preequilibrium process. Evaluation of light mass nuclei for JENDL PKA/KERMA file was being performed continuously.

References

1) Noda, K.: Proc. of 1994 Symposium on Nuclear Data, Tokai, Japan, Nov. 17-18, 1994, JAERI-Conf 95-008, p.112 (1995).
2) Baosheng, Y., et al.: J. Nucl. Sci. Technol., **29**, 677 (1992).
3) Nakagawa, T., et al.: ibid., **32**, 1259 (1995).
4) Lee, Y., Chang, J. and Fukahori, T.: J. Nucl. Sci. Technol., **35[10]**, 685 (1998).
5) Fukahori, T., et al.: Proc. of the Third Specialists' Meeting on Nuclear Data for Fission Reactors, Tokai, Japan, Nov. 29-30, 1995, JAERI-Conf 96-005, p.130 (1996).

Table 1.2.1 Neutron File up to 50 MeV for IFMIF

Compiling (40 nuclides)	H-1(< 1 GeV), C-12(< 80 MeV), Na-23, Mg-24,25,26, Al-27, Si-28,29,30, K-39, Ca-40,42,43,44,46,48, Ti-46,47,48,49,50, V-51, Cr-50,52,53,54, Mn-55, Fe-54,56,57,58, Ni-58,60,61,62,64, Cu-63,65, Y-89
Evaluating (23 nuclides)	Li-6,7, Be-9, B-10,11, N-14, O-16, K-41, V-50, Co-59, Mo-92,94,95,96,97,98,100, W-180,182,183,184,186, Au-197

Table 1.2.2 Neutron & Proton File up to 3 GeV (Total: 123 nuclides)

1st priority (42 nuclides)	H-1, C-12, N-14, O-16, Na-23, Al-27, Cr-50,52,53,54, Fe-54,56,57,58, Ni-58,60,61,62,64, Cu-63,65, Ta-181, W-180,182,183,184,186, Au-197, Hg-196,198,199,200,201,202,204, Pb-204,206,207,208, Bi-209, U-235,238
2nd priority (41 nuclides)	H-2, Mg-24,25,26, Si-28,29,30, K-39,41, Ca-40,42,43,44,46,48, Ti-46,47,48,49,50, V-51, Mn-55, Co-59, Zr-90,91,92,94,96, Nb-93, Mo-92,94,95,96,97,98,100, Pu-238,239,240,241,242
3rd priority (40 nuclides)	Li-6,7, Be-9, B-10,11, C-13, F-19, Cl-35,37, Ar-35,38,40, V-50, Zn-64,66,67,68,70, Ga-69,71, Ge-70,72,73,74,76, As-75, Y-89, Th-232, U-233,234,236, Np-237, Am-241,242,242m,243, Cm-243,244,245,246

Table 1.2.3 The nuclei to be included in the Photonuclear Data File

29 elements, 50 isotopes ^{2}H, ^{12}C, ^{14}N, ^{16}O, ^{23}Na, ^{24,25,26}Mg, ^{27}Al, ^{28,29,30}Si, ^{40,48}Ca, ^{46,48}Ti, ^{51}V, ^{52}Cr, ^{55}Mn, ^{54,56}Fe, ^{59}Co, ^{58,60,61,62,64}Ni, ^{63,65}Cu, ^{64}Zn ^{90}Zr, ^{93}Nb, ^{92,94,96,98,100}Mo, ^{133}Cs, ^{160}Gd, ^{181}Ta, ^{182,184,186}W, ^{197}Au, ^{206,207,208}Pb, ^{209}Bi, ^{235,238}U

Table 1.2.4 The elements to be included in the PKA/KERMA File

29 elements, 78 isotopes H, Li, Be, B, C, N, O, F, Na, Mg, Al, Si, Cl, K, Ca, Ti, V, Cr, Mn, Fe, Co, Ni, Cu, Zr, Ge, Nb, Mo, W, Pb, Bi

III-A-6 Systematics of Fission Cross Sections at the Intermediate Energy Region

T. Fukahori, O. Iwamoto, M. Mitsuhashi and S. Chiba

The fission cross section of actinide nuclei is one of the important physical quantities for radioactive waste transmutation. Calculation tools for this quantity in the intermediate energy region are still under development, except some codes such as ALICE and HETC. We have developed a semi-empirical formula for proton-induced fission cross section, which has rather more experimental data than the other particle induced cross sections. On the other hand, neutron-induced fission cross sections in the intermediate energy region have been systematically measured at Gatchina (Russia) and Los Alamos National Laboratory (U.S.). This report shows the semi-empirical formula previously developed has been expanded for neutron-, proton- and photon-induced fission cross sections simultaneously using new neutron-induced experimental data of ^{232}Th, ^{233,235,238}U and ^{237}Np, and the formula succeeded to explain most of experimental data.

The ***Z***- and ***A***-independent parameters, $\boldsymbol{q}_{i,j}$, has been fit by using experimental data for 29 isotopes from Ag to ^{243}Am with following formula;

$$\boldsymbol{P}_{fis}(\boldsymbol{Z}, \boldsymbol{A}, \boldsymbol{E}) = p_1[1 - \exp\{-p_3(E - p_2)\}]$$

$$p_1 = [1 + \exp\{(q_{1,1} - x)/q_{1,2}\}]^{-1}$$

$$p_i = \exp(q_{i,1} + q_{i,2}x) \qquad (i = 2,3)$$

$$x = Z^2 / A$$

where P_{fis} is fission cross section fraction to total reaction cross section ($=\sigma_{fis}/\sigma_R$), ***Z*** and ***A*** are atomic and mass number of compound nuclei, and ***E*** is excited energy.. The fitting results are shown in Table 1, and the "best-fit" parameters have a trend of good linearity. These results can derive that neutron-, proton- and photon-induced fission cross sections can be explained by only one formula. This formula can give not only the systematics for fission cross section at a certain energy point but also the shapes of excite function. Using this formula make possible to estimate the fission cross section for the nuclei for which few experimental data exist.

Table 1 Results of parameter fitting.

	p_1	p_2	p_3
$q_{i,1}$	-34.89	32.34	-0.8613
$q_{i,2}$	0.6502	-35.95	0.9473

III-A-7

Introduction of Model Calculated Beta-Ray Spectrum to ENDF/B-VI Fission Product Decay Data File

J. Katakura and T.R. England

A paper on this subject was presented at the International Conference on the Physics of Nuclear Science and Technology, on October 5 - 8, 1998, Long Island, New York, with following abstract.

ENDF/B-VI fission products decay data files are motivated to be used in applications. This motivation requires a complete data set of average decay energies and spectra. In order to provide the complete data model calculation is introduced in the B/VI fission product decay data file for nuclides with no measured data or incomplete ones. In this report the beta-ray spectra in the B/VI FP file and their comparison with measured ones including aggregate fission products spectra are presented.

B. Research Group for Hadron Science

III-B-1

Quantum molecular dynamics approach to the nuclear matter below the saturation density

T. Maruyama, K. Niita, K. Oyamatsu, T. Maruyama,
S. Chiba and A. Iwamoto

A paper on this subject was published in Phys. Rev. C 57, 655(1998) with the following abstract :

Quantum molecular dynamics is applied to study the ground state properties of nuclear matter at subsaturation densities. Clustering effects are observed to soften the equation of state at these densities. The structure of nuclear matter at subsaturation density shows some exotic shapes with variation of the density.

III-B-2

Nucleon interaction with ^{12}C studied by the soft-rotator model and a limit on the charge-symmetry breaking in the nuclear mean field

Efrem Sh. Sukhovitskij, Satoshi Chiba, Osamu Iwamoto
and Yurij V. Porodzinskij

A paper on this subject was published in Nuclear Physics A 640, 147(1998) with the following abstract :

The soft-rotator model was extended to include a capability to calculate the proton-nucleus scattering, and was used for a consistent analysis of the collective nuclear structure, EM transition and the nucleon (both neutron and proton) interaction data of ^{12}C. It was found that the model could describe these quantities to a good accuracy except for an anomalous behavior in the inelastic proton scattering to the first excited state at backward angles above the incident energy of 40 MeV. The difference in the neutron and proton real potential depths was used to infer the limit on the charge-symmetry breaking (CSB) in the nuclear mean field, which was found to be -5.7 $\pm$ 16.6 MeV fm^3, or (-0.6 $\pm$ 1.8)% of the nuclear mean field of ^{12}C. More precise neutron scattering data are highly desired because 1) the main source of the uncertainty for the CSB study came from the neutron interaction data, and 2) there is no neutron data corresponding to the anomaly in the proton inelastic scattering mentioned above.

III-B-3

Measurement and theoretical analysis of neutron elastic scattering and inelastic reactions leading to 3-body final state for ^{6}Li at 10 to 20 MeV region

S. Chiba, K. Togasaki, M. Ibaraki, M.Baba, S. Matsuyama, N.Hirakawa, K. Shibata, O. Iwamoto, A.J. Koning, G.M. Hale and M.B. Chadwick

A paper on this subject was published in Phys. Rev. C58, 2205(1998) with the following abstract :

The neutron elastic and inelastic scattering double-differential cross sections of ^{6}Li were measured at incident neutron energies of 11.5, 14.1 and 18.0 MeV. A phenomenological neutron optical model potential (OMP) of ^{6}Li was constructed to describe the total and elastic scattering cross sections from 5 MeV to several tens MeV, based on the present data together with information from other works. This potential was found to describe the inelastic scattering to the 1st excited state (Ex = 2.186 MeV) well via the DWBA calculation with the macroscopic vibrational model. The continuum neutron energy spectra and angular distributions were then analyzed by the theory of final-state interaction extended to the DWBA form, with an assumption that the d-α interaction is dominant in the 3-body final state consisting of n, d and α particles. Such a calculation was found to be successful in explaining the major part of the low-excitation neutron spectra and angular distribution down to the Q-value region of -9 MeV, except for the Q-value range where the n-α quasi-free scattering will give a non-negligible contribution at forward angles.

IV. Japan Nuclear Cycle Development Institute

A. Waste Management and Fuel Cycle Research Center

IV-A-1

Measurement of the Effective Neutron Capture Cross Section of ^{134}Cs by Triple Neutron Capture Reaction Method

T. Katoh[1)], S. Nakamura, H. Harada, Y. Hatsukawa[2)], N. Shinohara[2)], K. Hata[2)], K. Kobayashi[2)], S. Motoishi[2)] and M. Tanase[2)]

I. Introduction

The purpose of present experiment was to measure the effective neutron capture cross section($\hat{\sigma}$) of ^{134}Cs by using an activation method with a triple neutron capture reaction, ^{133}Cs(n, γ)^{134}Cs(n, γ)^{135}Cs(n, γ)^{136}Cs.

The reason for the use of the triple capture reaction is as follows. Since radioactive ^{134}Cs samples usually include the natural cesium(^{133}Cs), additional ^{134}Cs is produced from this natural cesium during the neutron irradiation of the targets and then the amount of ^{134}Cs in the targets becomes ambiguous. A high purity natural cesium(^{133}Cs) sample was, therefore, used for targets and ^{134}Cs produced through the neutron capture reaction of ^{133}Cs was used for the targets to make the amount of ^{134}Cs definite. The amount of ^{135}Cs which was produced by the neutron capture of ^{134}Cs was estimated from the activity measurement of ^{136}Cs induced by the reaction ^{135}Cs(n, γ)^{136}Cs since the ^{135}Cs emits a β-ray but no γ-ray. The values of cross sections of ^{133}Cs[(1)] and ^{135}Cs[(2)] obtained by the authors were used for the data analysis of the present measurement.

II. Experiment

1. Target Preparation

High purity(99.99%) cesium chloride powder was used for the targets. A 0.46 wt% Co/Al alloy wire was irradiated together with the Cs target to monitor the neutron flux. The thermal neutron flux and the epithermal component of the

1) Japan Nuclear Cycle Development Institute
and Gifu College of Medical Technology
2) Japan Atomic Energy Research Institute

neutron field of the reactor were measured by 0.112 wt% Au/Al alloy wires and 0.46 wt% Co/Al alloy wires.

2. Neutron Irradiation

The Cs target of about 2 μg was irradiated together with the Co/Al alloy wire for 23 days and 17 hours(long irradiation) in the HR-1 pipe of the swimming pool type reactor, JRR-3 at Japan Atomic Energy Research Institute(JAERI). The JRR-3 has a Maxwell spectrum in the thermal energy region and a 1/E spectrum in the epithermal energy region. After this irradiation, short irradiations for the Au/Al and Co/Al alloy wires were performed for 10 min in the HR-1 pipe to monitor the neutron field.

3. Activity Measurement

A high purity Ge detector was employed for the measurement of γ-rays from the irradiated target and monitor wires. The performance of the Ge detector was characterized as a 90% relative efficiency and 2.1 keV FWHM at the 1.33 MeV γ-peak of ^{60}Co. The irradiated target(or monitor wires) were set at the distance of 100 mm from the end-window of the Ge detector. The full energy peak efficiencies of the detector were calibrated with the standard γ-ray sources of ^{152}Eu and ^{133}Ba. The details of the data taking system were described elsewhere[(3)].

The γ-rays originating in the levels of ^{134}Ba and ^{136}Ba, which were the decay products of ^{134}Cs and ^{136}Cs nuclides induced by the single and the triple neutron capture reactions on ^{133}Cs, were seen at the energies of 796, 802, 819, 1039, 1048, 1168 and 1235 keV. Decays of the peak counts of the 819 and the 1048 keV γ-rays were followed. Their half-lives obtained were 12.6 ± 0.7 d for both of the 819 keV and the 1048 keV γ-rays. This value is in agreement with the value of half-life(12.63 ± 0.04 d) of ^{136}Cs obtained previously[(2)]. It was confirmed that the ^{136}Cs was produced through the triple neutron capture process from the ^{133}Cs.

III. Analysis

The numbers of ^{134}Cs and ^{136}Cs nuclei induced by the single and the triple neutron capture reactions of ^{133}Cs can be estimated as follows:

$$N_1 = N_0(0)R_0\left[\frac{\exp(-R_0t)-\exp\{-(R_1+\lambda_1)t\}}{(R_1+\lambda_1)-R_0}\right], \qquad (1)$$

$$N_3 = N_0(0)R_0R_1R_2[A_1 + A_2 + A_3], \quad (2)$$

where

$$A_1 = \frac{\exp(-R_0t) - \exp\{-(R_3 + \lambda_3)t\}}{\{(R_1 + \lambda_1) - R_0\}\{(R_2 + \lambda_2) - R_0\}\{(R_3 + \lambda_3) - R_0\}},$$

$$A_2 = \frac{\exp\{-(R_1 + \lambda_1)t\} - \exp\{-(R_3 + \lambda_3)t\}}{\{R_0 - (R_1 + \lambda_1)\}\{(R_2 + \lambda_2) - (R_1 + \lambda_1)\}\{(R_3 + \lambda_3) - (R_1 + \lambda_1)\}},$$

and

$$A_3 = \frac{\exp\{-(R_2 + \lambda_2)t\} - \exp\{-(R_3 + \lambda_3)t\}}{\{R_0 - (R_2 + \lambda_2)\}\{(R_1 + \lambda_1) - (R_2 + \lambda_2)\}\{(R_3 + \lambda_3) - (R_2 + \lambda_2)\}}.$$

Here, the $N_0(0)$ means the number of ^{133}Cs nuclei included in the target at the time of start of irradiation, and N_1 and N_3 are the numbers of ^{134}Cs and ^{136}Cs nuclei, respectively. The reaction rates of neutron capture by ^{133}Cs, ^{134}Cs, ^{135}Cs and ^{136}Cs are shown by R_0, R_1, R_2 and R_3, respectively. The decay constants of ^{134}Cs, ^{135}Cs and ^{136}Cs are expressed by λ_1, λ_2 and λ_3, respectinely. The irradiation period is represented by t.

In the present study, a relation between the activity ratio($\lambda_3N_3/(\lambda_1N_1)$) of ^{136}Cs and ^{134}Cs and the effective neutron capture cross section($\hat{\sigma}$) of ^{134}Cs was calculated numerically by using Eqs.(1) and (2), In this calculation, each reaction rate(R's) was estimated from a relation, $R=nv_0\hat{\sigma}$, in which nv_0 was replaced by the thermal flux measured for the present neutron field. The effective neutron cross section for each nuclide except for ^{134}Cs was calculated from the cross section and the resonance integral of each nuclide. Data for ^{133}Cs[(1)] and ^{135}Cs[(2)] were those measured previously by the present authors. The decay constant was calculated from half-live of each nuclide.

The effective neutron capture cross section, $\hat{\sigma}$, for ^{134}Cs was deduced by inserting the measured value of the activity ratio($\lambda_3N_3/(\lambda_1N_1)$) of ^{136}Cs and ^{134}Cs into the relation calculated. Experimental activity ratios were obtained from peak counts ratios of γ-rays from ^{136}Cs and ^{134}Cs taken in the same spectrum. Since the peak counts ratio of γ-rays was used for the analysis, correction for solid angle of detector was not necessary and relative detection efficiency(not absolute detection efficiency) was enough for the deduction of activity ratio. The $N_0(0)$ was cancelled in the activity ratio. The absolute intensity of activity in the target was not necessary.

IV. Results

The effective neutron capture cross section for ^{134}Cs obtained in the present measurement was 140.6 ± 8.5 barns. The present value was in agreement with that by Bayly et al. [4]

As for the measurement of the resonance integral, the possibility of experiment with the same method was estimated. For this purpose, neutron irradiation of sample in a Cd shield capsule is required. However, estimation in advance shows that the activity of ^{136}Cs produced by the neutron irradiation within a Cd shield capsule is several orders smaller than that produced by the irradiation without a Cd shield, and it was found that the measurement of resonance integral by this method is impossible. Other method must be designed to measure the resonance integral of the reaction $^{134}Cs(n, \gamma)^{135}Cs$.

ACKNOWLEDGMENT

The authors wish to acknowledge their indebtedness to Drs. S. Nomura and H. Funasaka of Japan Nuclear Cycle Development Institute(JNC) for their interest and encouragement in this work. Thanks are also due to the crew of the JAERI Reactor(JRR-3) for their cooperation.

This work was supported by JNC, JAERI and Inter-University Program for the Joint Use of JAERI Reactor.

REFERENCES

(1) Nakamura, S., Harada, H., Katoh, T.: *J. Nucl. Sci. Technol.*, to be published.

(2) Katoh, T., Nakamura, S., Harada, H., Hatsukawa, Y., Shinohara, N., Hata, K., Kobayashi, K., Motoishi, S., Tanase, M.: *J. Nucl. Sci. Technol.,* **34**, 431 (1997).

(3) Harada, H., Nakamura, S., Katoh, T., Ogata, Y.: *J. Nucl. Sci. Technol.*, **32**, 395 (1995).

(4) Bayly, J. G., Brown, F., Hall, G. R., Walter, A. J.: *Inorg. Nucl. Chem.*, **5**, 259 (1958).

IV-A-2

High-Resolution Measurement of Fine Structure in the Photoabsorption Cross Section of 18O

H. Harada, Y. Shigetome, H. Ohgaki[1], T. Noguchi[1] and T. Yamazaki[1]

A paper on this subject was published in Phys. Rev. Lett. 80, 33 (1998), with the following abstract.

A new experimental method for the high-resolution measurement of photoabsorption cross sections has been developed. The energy resolution of about 0.1% is achieved by measuring the transmitted photons from a target with a high-resolution high-energy photon spectrometer. The method is applied to the measurement of the photoabsorption cross section of ^{18}O in the giant resonance region. Significant fine structure of the resonance is observed.

[1]Electrotechnical Laboratory

IV-A-3

Super High Resolution Measurement of Fine Structure in the Total Photonuclear Cross Section of 13C

H. HARADA, K. FURUTAKA, Y. SHIGETOME, H. OHGAKI[1], and H. TOYOKAWA[1]

A paper on this subject was published in J. Nucl. Sci. Technol. 35, 733 (1998), with the following abstract.

The high-resolution data of photonuclear cross sections in the giant resonance (GR) region are important for the deep understanding of the GR. The data have also great impact on the innovative applications of photonuclear reactions because the photonuclear cross sections of some special states, especially sharp resonant states, are expected to have huge values that is comparable to the photoatomic cross sections. For example, the reaction can be used for selective isotope production, selective nuclear transmutation, and non-destructive isotope analysis when monochromatic photon sources become available.

To improve the energy resolution of the measurement on the photonuclear cross section, the photon attenuation method using a high-resolution high-energy photon spectrometer (HHS) and laser Compton photons (LCPs) has been proposed[1]. The HHS was designed to measure high-energy photons, typically 10-30 MeV, with an energy resolution of about 0.1 % and with high photopeak-to-background ratio. The method has been first applied to the measurement of the photoabsorption cross section of ^{18}O in the GR region[2]. Although the significant fine structure of the resonances has been observed in ^{18}O, the high-resolution performance of HHS could not be fully exploited due to moderate sharpness of the fine structure peaks observed in ^{18}O. This paper demonstrates the energy resolution of 0.1 % of this method by measuring the photon attenuation in the ^{13}C target where the narrow level width (5.5 keV) is known at the excitation energy of 15.11 MeV[3,4] from the ^{9}Be+α $\rightarrow$ ^{13}C (first T=3/2) resonance reaction.

References:

[1] Harada, H., Sigetome, Y. : J. Nucl. Sci. Technol. **32**, 1189 (1995).
[2] Harada, H., et al. : Phys. Rev. Lett. **80**, 33 (1998).
[3] Hinterberger, F., et al. : Nucl. Phys. **A308**, 61 (1978).
[4] Ajzenberg-Selove, F. : Nucl. Phys. **A523**, 1 (1991).

---

[1]Electrotechnical Laboratory

IV-A-4

Construction of a γ-γ and β-γ Coincidence Measurement System for Precise Determination of Nuclear Data

K. Furutaka, S. Nakamura, H. Harada and T. Katoh

A paper on this subject was published in Proc. the 1998 Nuclear Data Symposium with the following abstract.

A γ-γ and β-γ coincidence measurement system was constructed for the precise determination of nuclear data, such as thermal neutron capture cross sections and γ-ray emission probabilities. The validity of the system was tested by a γ-γ coincidence measurement with a ^{60}Co standard source.

IV-A-5

Calculation of Photonuclear Process in the Region of Several Tens MeV

- Formulation of Exact Transition Rate for High Energy γ-Ray -

Hiroaki Wada and Hideo Harada

A paper on this subject will be published in Proc. the 1998 Nuclear Data Symposium, Nov. 19-20, 1998, JAERI Tokai, with the following abstract.

The electromagnetic field approximated by using long wave-length limit is not valid for heavy nuclear mass or high energy γ-ray transition. To examine the contribution of the electric multipole field that is neglected in long wave-length limit, we formulize the *El* transition rate for the strict electric multipole field and compare quantitatively this result with Weisskopf estimate.

IV-A-6

Measurements of Thermal Neutron Capture Cross Sections for some FP Nuclides

Shoji NAKAMURA, Kazuyoshi FURUTAKA, Hideo HARADA and Toshio KATOH

A paper on this subject will be published in Proceedings of the 1998 Symposium on Nuclear Data, Nov. 19-20, 1998, JAERI Tokai, with the following abstract.

The thermal neutron capture cross sections (σ_0) and the resonance integrals (I_0) of some FP elements, such as ^{80}Se, ^{94}Zr, ^{124}Sn, ^{127}I and ^{133}Cs, were measured by the activation and γ-ray spectroscopic method.

V. Kyoto University

A. Research Reactor Institute

V-A-1

Measurement of Fission Cross Section of Pa-231 using Lead Slowing-down Spectrometer

Katsuhei Kobayashi[1], Shuji Yamamoto[1], Tetsuya Kai[1*], Hyun-Je Cho[1**], Hajimu Yamana[1], Yoshiaki Fujita[1], Toshiaki Mitsugashira[2], and Itsuro Kimura[3]

1 Research Reactor Institute, Kyoto University
Kumatori-cho, Sennan-gun, Osaka 590-0494, Japan
* Present address: Japan Atomic Energy Research Institute
Tokai-mura, Naka-gun, Ibaraki 319-1195, Japan
** Visiting Scientist from University of Ulsan, Korea
2 The Oarai-branch, Institute for Material Researche, Tohoku University,
Oarai-machi, Higashiibaraki-gun, Ibaraki 311-1313, Japan
3 Department of Nuclear Engineering, Kyoto University
Yoshida-honmachi, Sakyo-ku, Kyoto 606-8501, Japan

A paper on this subject was presented at the 1998 Symposium on Nuclear Data at Tokai-mura, JAERI held on Nov.19-20, 1998.

Making use of a back-to-back type double fission chamber and Kyoto University Lead slowing-down Spectrometer (KULS) driven by a 46 MeV electron linear accelerator (linac) at the Research Reactor Institute, Kyoto University (KURRI), the neutron- induced fission cross section of Pa-231 has been measured from 0.1 eV up to 10 keV with energy resolution (FWHM) of about 40 %. The cross section of the $^{235}U(n,f)$ reaction in ENDF/B-VI was used as a reference one for the measurement of the fission cross section. The measured result has been compared with the evaluated data in ENDF/B-VI, JENDL-3.2 and JEF-2.2, whose data were broadened by the energy resolution of the KULS. The ENDF/B-VI and the JEF-2.2 data almost overlap above 0.1 eV and the later is slightly lower than the former below 0.1 eV. Both evaluated data are lower below 0.15 eV and are higher near the bump of 5 eV and above about 20 eV than the measurement. To the contrary, the JENDL-3.2 data are lower than the measured result above about 100 eV, although the evaluated values are close to the current ones at lower energies.

V-A-2

Measurement of Neutron Capture Cross Sections of Dy and Hf In the Energy Region from 0.003 eV to 50 keV

Hyun-Je Cho[1*], Katsuhei Kobayashi[1], Shuji Yamamoto[1], Yoshiaki Fujita[1], Guinyun Kim[2], In Soo Ko[2], Moo-Hyun Cho[2], Won Namkung[2], Jonghwa Chang[3], and Seung Kook Ko[4]

1 Research Reactor Institute, Kyoto Universty
Kumatori-cho, Sennan-gun, Osaka, 590-0494, Japan
2 Pohang Accelerator Laboratory, POSTECH
San 31, Hyojadong Namgu, Pohang, 790-784, Korea
3 Korea Atomic Energy Research Insutute, KAERI
P.O. Box 105, Taejeon, 305-600, Korea
4 Department of Physics, University of Ulsan
San l, Moogedong, Namgu, Ulsan, 680-749, Korea
* Visiting Scientist from University of Ulsan, Korea

A paper on this subject was presented at the 1998 Symposium on Nuclear Data at Tokai-mura, JAERI held on Nov. 19-20, 1998.

The capture cross sections of Dy and Hf were measured in the energy region from 0.003 eV to 50 keV by the neutron time-of-flight method with a 46 MeV electron linear accelerator of the Research Reactor Institute, Kyoto University. An assembly of $Bi_4Ge_3O_{12}$ (BGO) scintillators, which was placed at a distance of 12.7 ± 0.02 m from the neutron source, was employed as a total energy absorption detector for the prompt capture gamma-ray measurement from the sample. In order to determine the neutron flux impinging on the capture sample, the Sm(n,γ) reaction was used for thermal neutrons and the $^{10}B(n,\alpha)$ reaction for neutrons from 0.003 eV to 50 keV.
Absolute capture yield for the sample was obtained from the saturated resonance data at a large resonance of the sample.

For the capture cross section of Dy, the existing experimental data and the evaluated data in ENDF/B-VI and JEF-2 are close to the present result. For the Hf cross section, the previous experimental data and the evaluated data in JENDL-3.2, ENDF/B-VI and JEF-2 are in general agreement with the present measurement.

V-A-3

Fission Cross Section Measurement for Am-242m with TOF Methods in Low Energy Region

Tetsuya Kai*[1], Katsuhei Kobayashi[1], Shuji Yamamoro[1], Cho Hyun-Je[1],
Yoshiaki Fujita[1], Itsuro Kimura[2], Yasushi Ohkawachi[3] and Toshio Wakabayashi[3]

1 Research Reactor Institute, Kyoto University
2 Department of Nuclear Engineering, Kyoto University
3 Japan Nuclear Cycle Development Institute
* Present Affiliation: Japan Atomic Energy Research Institute

A paper on this subject was presented at the 1998 Symposium on Nuclear Data at Tokai-mura, JAERI held on Nov. 19-20, 1998.

The neutron-induced fission cross section for Am-242m was measured with time-of-flight(TOF) method from 0.003 eV to 30 eV. We already measured the cross section using Kyoto University lead slowing-down spectrometer(KULS) from 0.1 eV to 10 keV and using the standard thermal neutron field (D_2O facility) at 0.025 eV. The measurement with TOF method was made for the purpose of the discussion about systematic difference of the results with the different experimental methods.

The measurement with TOF method was made using the 46 MeV electron linac at Kyoto University Research Reactor Institute. The pulsed neutron produced at the water-cooled tantalum(Ta) target as a result of electron beam irradiation are taken out from the reentrant hole in the center of the water tank (aluminum, $50\times40\times50$ cm^3). The sample deposit(Am-242m) and the reference one (U-235) was set in the back-to-back type double fission chamber, and the chamber was placed at approximately 5 m from the Ta target. The absolute value of the fission cross section for Am-242m was measured relative to that for U-235 from 0.003 eV to 1 eV. In order to avoid the resonance interference between Am-242m and U-235, the relative fission cross section measurement was made using a BF_3 counter instead of the U-235 fission chamber from 0.2 eV to 10 eV and was normalized to the absolute value measured relative to U-235 between 0.2 eV and 1 eV. The typical operating conditions of the linac during this measurement were as follows: pulse repetition of 80 Hz, pulse width of 22 ns, electron average current of $\sim 75\mu$s, and the energy of $\sim$ 31 MeV.

The present result, the thermal neutron-induced fission cross section measured using the D_2O facility and the evaluated data of the JENDL-3.2 and the ENDF/B-VI are compared. At 0.025 eV, although the present result and the value obtained with the D_2O facility agree in their experimental error, the JENDL-3.2 and the ENDF/B-VI are slightly larger than our results. In higher energy region ($>\sim$2 eV), the ENDF/B-VI data is much higher than the present result and the JENDL-3.2. The result with the TOF method and that with the KULS are compared with the evaluated data. For the comparison, the TOF result and the evaluated data are broadened with the energy resolution of the KULS. Since good agreement can be seen between the TOF result and the KULS result in the energy region lower than $\sim$0.2 eV, the thermal fission cross section obtained with the standard thermal neutron field is also consistent with the result measured using the KULS.

B. Department of Nuclear Engineering

V-B-1

Multi-parametric Measurement of Prompt Neutrons and Fission Fragments for $^{233}U(n_{th},f)$

K.Nishio, M.Nakashima, I.Kimura[1] and Y.Nakagome[2]

A paper on this subject was published in J. Nucl. Sci. and Technol. [1] and related three papers were also published [2] [3] [4].

The multiplicity and the energy of prompt neutrons from the fragments for $^{233}U(n_{th},f)$ were measured as functions of fragment mass and total kinetic energy. Average neutron energy against the fragment mass showed a nearly symmetric distribution about the half mass division with two valleys at 98 and 145 u. This shape formed a contrast with a saw-tooth distribution of the average neutron multiplicity. It indicates that the shell-effects, which are pronounced for the fragments having the proton number or neutron number close to the magic-number of 50 or 82, affected the neutron emission process. The slope of the neutron multiplicity with total kinetic energy depended on the fragment mass and showed the minimum at about 130 u. The obtained neutron data were applied to determine the total excitation energy of the system, and the resulting value in the typical asymmetric fission lied between 22 and 25 MeV. The excitation energy agreed with that determined by subtracting the total kinetic energy from the Q-value within 1 MeV, thus satisfied the energy conservation. In the symmetric fission , where the mass yield was drastically suppressed, the total excitation energy is significantly large and reaches to about 40 MeV, suggesting that fragment pairs are preferentially formed in a compact configuration at the scission point.

References ;

[1] K. Nishio, M. Nakashima, I. Kimura, Y. Nakagome, J. Nucl. Sci. Technol., **35** (1998) 631.

[2] K. Nishio, Y. Nakagome, H. Yamamoto, I. Kimura, Nucl. Phys., **A632** (1998) 540.

[3] K. Nishio, I. Kimura, Y. Nakagome, J. Nucl. Sci. Technol., **34** (1997) 439.

[4] K. Nishio, H. Yamamoto, I. Kanno, I. Kimura, Y. Nakagome, Nucl. Inst. Meth., **A385** (1997) 171.

---

1. Corresponding E-mail : kimura@nucleng.kyoto-u.ac.jp

2. Research Reactor Institute, Kyoto University

VI. Kyushu University

A. Department of Advanced Energy Engineering

VI-A-1

Helium Production Cross Section Measurement of Pb and Sn for 14.9MeV Neutrons

Y. Takao, T. Fujimoto, S. Ozaki, M. Muramasu, H. Nakashima, Y. Kanda*, and Y. Ikeda**

A paper on this subject was presented at the 1997 Symposium on Nuclear Data, and published in JAERI-Conf 98-003, p.180 (1998), with the following abstract:

Helium production cross sections of lead and tin for 14.9 MeV neutrons were measured by helium accumulation method. Lead and tin samples were irradiated with FNS, an intense d-T neutron source of JAERI. The amount of helium produced in the samples by the neutron irradiation was measured with the Helium Atoms Measurement System (HAMS) at Kyushu University. As the samples contained a small amount of helium because of their small helium production cross sections at 14.9 MeV, the samples were evaporated by radiation from a tungsten filament to decrease background gases at helium measurement. Uncertainties of the present results were less than ±4.4%. The results were compared with other experimental data in the literature and also compared with the evaluated values in JENDL-3.2.

* Oita National College of Technology
** Department of Reactor Engineering, Japan Atomic Energy Research Institute

VI-A-2

Improvements on semi-classical distorted-wave model

Sun Weili, Y. Watanabe, R. Kuwata, M. Kohno†, K. Ogata‡, and M. Kawai‡

A paper on this subject was presented at the 1997 Symposium on Nuclear Data, and published in JAERI-Conf 98-003 (1998) pp.282–287, with the following abstract:

A method of improving the Semi-Classical Distorted Wave (SCDW) model in terms of the Wigner transform of the one-body density matrix is presented. Finite size effect of atomic nuclei can be taken into account by using the single particle wave functions for harmonic oscillator or Woods-Saxon potential, instead of those based on the local Fermi-gas model which were incorporated into previous SCDW model. We carried out a preliminary SCDW calculation of 160 MeV $(p,p'x)$ reaction on ^{90}Zr with the Wigner transform of harmonic oscillator wave functions. It is shown that the present calculation of angular distributions increase remarkably at backward angles than the previous ones and the agreement with the experimental data is improved.

† Physics Division, Kyushu Dental College
‡ Department of Physics, Kyushu University

VI-A-3

Study of the p+^{12}C reaction at energies up tp 30 MeV

M. Harada, A. Yamamoto, S. Yoshioka, K. Sato, T. Nakashima, H. Ijiri, Y. Watanabe, H. Yoshida*, Y. Uozumi*, S. Chiba**, T. Fukahori**, S. Meigo**, and O. Iwamoto**

A paper on this subject was presented at the 1997 Symposium on Nuclear Data, and published in JAERI-Conf 98-003 (1998) pp.276–281, with the following abstract:

Double differential cross sections of charged-particles emitted in the p+^{12}C reaction were measured in the energy region from 14 to 26 MeV. The observed continuous components of emitted protons and α-particles were analyzed by assuming sequential decay of intermediate reaction products and/or simultaneous breakup process. It was found that the three body simultaneous decay, p + α + ^{8}Be, and the sequential decay via p + ^{12}C$^{*}_{3^-}$ and α + ^{9}B$_{g.s.}$ are most important in the proton-induced breakup of ^{12}C for energies up to 30 MeV

* Department of Nuclear Engineering, Kyushu University
** Japan Atomic Energy Research Institute

VI-A-4

In-medium nucleon-nucleon cross sections from nonrelativistic reaction matrices in nuclear matter

M. Kohno†, M. Higashi, Y. Watanabe, and M. Kawai‡

A paper on this subject was published in *Phys. Rev.* C **57**, No.6, pp. 3495–3498 (1998), with the following abstract:

In-medium nucleon-nucleon cross sections are calculated from reaction matrices of the nonrelativistic Brueckner approach. Calculated cross sections are parametrized as a function of the incident energy and the nuclear density. The nonrelativistic cross sections are found to be reduced from free ones as observed in relativistic Brueckner calculations. This reduction of the in-medium cross sections is ascribed to the flux renormalization represented by an effective mass. It is pointed out that we should be careful to avoid double counting the effective mass effects when in-medium cross sections calculated are applied in various models of dynamical nuclear processes.

† Physics Division, Kyushu Dental College
‡ Department of Physics, Kyushu University

VI-A-5

Development of low threshold ΔE-E Counter Telescope for (p, α) reaction experiment

A. Yamamoto, M. Harada, H. Ijiri, and Y. Watanabe

A paper on this subject was published in Engineering Sciences Reports, Kyushu University (KYUSHU DAIGAKU SOGORIKOGAKU KENKYUKA HOKOKU) Vol. 20, No. 2, pp. 151–156 (1998), with the following abstract:

We have developed a compact ΔE-E counter telescope composed of a proportinal gas-counter as the ΔE detector and a silicon surface barrier detector as the E detector in order to measure energy spectra of emitted α particles from proton-induced reactions on ^{12}C. A thin window made of aluminum-evaporated mylar foil and low pressure P-10 gas were employed in the ΔE counter to achieve the low threshold energy of detected α particles by reducing the energy loss in the ΔE counter. The developed counter telescope has been used successfully in an experiment of the ^{12}C(p, α) reaction at incident energies of 14 and 18 MeV, and the threshold energy of α particles was about 1 MeV.

VI-A-6

Status of experimental data of proton-induced reactions for intermediate-energy nuclear data evaluation

Y. Watanabe, T. Kawano, N. Yamano*, and T. Fukahori**

A paper on this subject was presented at the Third Specialists' Meeting on High Energy Nuclear Data, March 30–31, 1998, JAERI, Tokai, and published in JAERI-Conf 98-016 (1998) pp.16–29, with the following abstract:

The present status of experimental data of proton-induced reactions is reviewed, with partcular attention to total reaction cross section, elastic and inelastic scattering cross section, double-differential particle production cross section, isotope production cross section, and activiation cross section.

* Department of Nuclear Design, Sumitomo Atomic Energy Industries, Ltd.
** Nuclear Data Center, Japan Atomic Energy Research Institute

VI-A-7

Master equation approach to statistical multistep compound reactions

T. Kawano, M. Nakamura, and Y. Watanabe

A paper on this subject was partly published in *Proc. Int. Conf. on Nuclear Data for Science and Technology*, 19–24 May, 1997, Trieste, Italy, (1998) p.348, and the complete paper was published in *Phys. Rev.* C **57**, 978 (1998), with the following abstract:

A master equation is incorporated in Feshbach, Kerman, and Koonin model calculations of statistical multistep compound (MSC) emission. Damping X and Y functions which describe the particle-hole annihilation process are derived. The MSC cross sections are calculated with the master equation. The effect was found to be large at lower energies for light nuclei, but not significant when the incident energy is above 20 MeV. The difference between a closed form solution and the master equation result is masked by the large multistep direct and evaporation components.

VI-A-8

Microscopic calculation of the multistep compound process

T. Kawano

A paper on this subject was partly published in JAERI-Conf 98-003 (1998) pp.312–317, and the complete paper will be published in *Phys. Rev.* C **59**, (1999) with the following abstract:

The Feshbach, Kerman, and Koonin model of statistical multistep compound (MSC) process is calculated microscopically, and comparisons of the microscopically calculated MSC process with a phenomenological phase-space model are made. The microscopic model gives a small particle emission probability in comparison with the constant wave function approximation, and a simple way to reconcile the difference is proposed. A $2p$-$1h$ doorway state formation cross section is calculated with the spherical Nilsson model, and a strength of the residual interaction V_0 is estimated from the doorway state formation cross section. The obtained V_0 is of the same magnitude as those derived in the previous multistep direct analyses. Comparisons of the microscopic MSC calculations with the experimental data show that the calculated particle emission spectra reproduce the measurements at backward angles.

VI-A-9

Validity of DWBA Calculations for Neutron Inelastic Scattering from Molybdenum Isotopes

T. Kawano, Y. Watanabe, and M. Kawai*

A paper on this subject was published in *J. Nucl. Sci. Technol.*, **35**, 519 (1998) with the following abstract:

Neutron inelastic scattering cross sections for molybdenum isotopes are calculated with the DWBA and the coupled-channels methods. Anomalous enhancement of the DWBA cross sections near the threshold energy appears when the adopted optical potential has a shallow imaginary part. Calculations with some simplified optical potentials indicate that the enhancement can be related with the p-wave strength, and it is found that the problem comes from the optical potential used.

When an adopted optical potential to the DWBA calculation is physically reasonable, differences between the calculated cross sections with the DWBA and those with the coupled-channels theory are small. Experimental data of ^{92}Mo, ^{98}Mo and ^{100}Mo are well reproduced by the calculated cross sections with the DWBA and the Hauser-Feshbach-Moldauer statistical model, and it is concluded that the DWBA is an appropriate method to evaluate cross sections of inelastic scattering from the molybdenum isotopes.

* High Energy Accelerator Research Organization

VII. Nagoya University

A. Department of Energy Engineering and Science

VII-A-1

Measurement of Q_{EC} values of ^{126}La isomers

Y. Kojima, M. Asai, A. Osa[1], M. Koizumi[1], T. Sekine[1],
M. Shibata, H. Yamamoto and K. Kawade

A paper on this subject was published in Appl. Radiat. Isot. 49, 829-834(1998).

Beta-ray endpoint energies of the neutron-deficient nuclide of ^{126}La have been measured with an HPGe detector. The ^{126}La activities were produced by the ^{94}Mo (^{36}Ar, 3pn) reaction and mass-separated on-line. From the β-γ coincidence measurements, Q_{EC}-values of the high- and low- spin isomers of ^{126}La were determined for the first time to be 7700(100) keV and 7910(400) keV, respectively. The experimental atomic masses were compared with predicted values of mass formulas.

---

[1]Japan Atomic Energy Research Institute

VII-A-2

Q_{EC} measurement of $^{124,125,127\text{-}130}$La

Y. Kojima, M. Asai, A. Osa[1], M. Koizumi[1], T. Sekine[1],
M. Shibata, H. Yamamoto, K. Kawade and T. tachibana[2]

A paper on this subject was published in J. Phys. Soc. Jpn 67, 3405-3413(1998).

For the neutron-deficient Q_{EC} measurement of $^{124,125,127\text{-}130}$La has been performed by determining β^+–ray maximum energies. The radioactive sources were prepared by on-line mass-separation following the fusion-evaporation reactions ^{92,nat}Mo(^{36}Ar, 3pxn). The β^+-rays were measured with an HPGe detector in β-γ coincidence mode in which γ-rays were detected with another HPGe detector for specifying an excited state in daughter nucleus. By unfolding the β^+-ray spectra using experimental response functions, the Q_{EC}-values of $^{124,125,127\text{-}130}$La were newly obtained, and those of ^{128,129}La were improved in their accuracy. The Q_{EC}-values obtained and the resulting atomic masses are compared with theoretical predictions. The results of half-life calculation and two-neutron separation energies using the experimental Q_{EC}-values are also discussed.

[1]Japan Atomic Energy Research Institute
[2]Advanced Research Institute for Science and Engineering, Waseda University

VII-A-3

Beta-decay half-lives and level ordering of $^{102m,g}Rh$

M. Shibata, Y. Satoh, S. Itoh, H. Yamamoto, K. Kawade,
Y. Kasugai[1] and Y. Ikeda[1]

A paper on this subject was published in Appl.Radiat.Isot. 49, 1481-1487(1998).

Beta-decay half-lives of the ground state and an isomer of ^{102}Rh have been determined 207.3(17) d and 3.742(10) y, respectively, by γ-ray decay curves following each β-decay. It has been found that a state (2$^-$) which has a shorter half-life (207.3d) is the ground state from the result that the half-life of the 41.9 keV isomeric γ-transition was equal to 3.742 y. It has also been confirmed that the 41.9 keV transition is certainly an isomeric transition with X-γ coincidence measurement.

[1]Japan Atomic Energy Research Institute

VII-A-4

Measurement of (n,p) cross sections for short-lived products by 13.4 - 14.9 MeV neutrons

Y. Kasugai[1], H. Yamamoto, K. Kawade and T. Iida[2]

A paper on this subject was published in Ann. Nucl. Energy 25, 23-45(1998).

The 28 (n,p) activation cross sections leading to short-lived nuclei with half-lives between 20 s and 18 min were measured in the energy range between 13.4 and 14.9 MeV by activation method. The measured isotopes were ^{19}F, $^{28,29}Si$, ^{37}Cl, ^{50}Ti, $^{52,53,54}Cr$, $^{60,62}Ni$, $^{66,68}Zn$, $^{86,88}Sr$, ^{97}Mo, $^{101,102,104}Ru$, $^{104,105,108}Pd$, ^{107}Ag, ^{116}Cd and $^{119,120}Sn$. The intense 14 MeV neutron source facility (OKTAVIAN) at Osaka University was used for irradiation. The γ-rays emitted from the irradiated samples were measured with high-purity germanium (HPGe) detectors. All cross section values were obtained relative to the standard reaction cross section of $^{27}Al\ (n,\alpha)\ ^{24}Na$. The present results were compared with previous data and the evaluated data of JENDL-3 and ENDF/B-VI. Ten reactions have been obtained at multi-point-energies for the first time. By using intense neutron sources and making careful corrections, reliable results could be obtained. Most of previous data obtained at multi-point-energies have shown reasonable agreement within 25%. In comparison of experimental 10 reactions with the evaluated data, significant discrepancies more than 25% have been seen for 3 reactions.

---

[1]Present address; Japan Atomic Energy Research Institute.
[2]Department of Electronic, Information Systems and Energy Engineering, Osaka University

VII-A-5

Systematics for (n,α) excitations in the neutron energy between 13.3 and 15.0 MeV

Y. Kasugai[1], Y. Ikeda*, H. Yamamoto and K. Kawade

A paper on this subject was published in Ann. Nucl. Energy 25, 421-435(1998).

Systematics of (n,α) excitation functions in the neutron energy between 13.3 and 15.0 MeV were studied on the basis of experimental data measured by the Nagoya University and FNS groups (Japan Atomic Energy Research Institute). The empirical formulae of cross sections at 14.0 MeV (σ_{14}) and relative slopes of excitation functions (S) were deduced. These formulae covered the mass range between 19 and 188. The empirical formula of relative slope was expressed as a function effective threshold energy $E_{th}+V_\alpha$, where Eth is threshold energy and V_α is Coulomb barrier for α-particle emitted from the compound nucleus. The empirical formula of σ_{14} was expressed by a simple formula with two fitting parameters. By using the proposed empirical formulae, the partial excitation functions between 13 and 15 MeV were reproduced. Comparing the experimental data with the calculated excitations, we concluded that the accuracy of the proposed empirical formulae was ±30%.

[1]Present address; Japan Atomic Energy Research Institute
*Japan Atomic Energy Research Institute

VII-A-6

Measurement of (n,α) cross sections for short-lived products by 13.4 - 14.9 MeV neutrons

Y. Kasugai[1], H. Yamamoto, K. Kawade and T. Iida[2]

A paper on this subject was published in Ann.Nucl.Energy 25, 485-1502 (1998).

Twelve (n,α) activation cross sections leading to short-lived nuclei with half-lives between 37 s and 15 min were measured in the energy range between 13.4 and 14.9 MeV by activation method. The measured reactions involved the isotopes of ^{26}Mg, ^{31}P, ^{54}Cr, ^{63}Cu, ^{64}Ni, ^{69}Ga, ^{71}Ga, ^{87}Ru, ^{89}Y, ^{104}Ru and ^{112}Cd. The intense 14 MeV neutron source facility (OKTAVIAN) at Osaka University was used for irradiation. The γ-rays emitted from the irradiated samples were measured with high-purity germanium (HPGe) detectors. All cross section values were obtained relative to the standard reaction cross section of ^{27}Al (n, α) ^{24}Na. The cross sections of 4 reactions were measured for the first time. The present experimental data were discussed by comparing with previously reported experimental data and the evaluated data of JENDL-3 and ENDF/B-VI. The 6 evaluated data in JENDL-3 shows reasonable agreement within 7%, but the evaluation of ^{26}Mg reaction is 25% higher than our data. The 2 evaluation data of ENDF/B-VI agree well, but one evaluation is deviated more than 25% have been seen for 3 reactions.

[1]Present address; Japan Atomic Energy Research Institute.
[2]Department of Electronic, Information Systems and Energy Engineering, Osaka University

VII-A-7

Can the equation of state of asymmetric nuclear matter be studied using unstable nuclei?

K. Oyamatsu [a,b], I. Tanihata [a], Y. Sugahara [a], K. Sumiyoshi [a] and H. Toki [a,c]

[a] *The Institute of Physical and Chemical Research (RIKEN) Hirosawa, Wako, Saitama 351-01, Japan*

[b] *Department of Energy Engineering and Science, Nagoya University Furo-cho, Chikusa-ku, Nagoya, 464-01, Japan*

[c] *Research Center for Nuclear Physics (RCNP), Osaka University Mihogaoka, Ibaraki, Osaka, 567, Japan*

A paper on this subject was published in Nucl. Phys. **A634**, 3-14 (1998) with the following abstract.

This paper shows that nuclear radii and neutron skins do directly reflect the saturation density of asymmetric nuclear matter. The proton distributions in a nucleus have been found to be remarkably independent of the equation of state (EOS) of the asymmetric matter. It is the neutron distributions that are dependent on the EOS. Macroscopic model calculations have been performed over the entire range of the nuclear chart based on two popular phenomenological, but distinctively different, EOS : the SIII parameter set for the non-relativistic Skyrme Hartree-Fock theory and the TM1 parameter set in the relativistic mean field theory. The saturation density for a small proton fraction remains almost the same as the normal nuclear matter density for SIII EOS, but it becomes significantly small for the TM1 EOS. The key EOS parameters used to describe the saturation density are the density derivative of the symmetry energy and the incompressibility of symmetric nuclear matter, while the saturation energy is written using the symmetry energy alone as a good approximation. We conclude that a systematic experimental study of heavy unstable nuclei would enable us to determine the EOS of asymmetric nuclear matter at about the normal nuclear matter density with a fixed proton fraction down to about 0.3.

VII-A-8

Intercomparison of delayed neutron summation calculations among JEF2.2, ENDF/B-VI and JNDC-V2

M.Sagisaka, K.Oyamatsu, Y.Kukita

A paper on this subject was published in Proc. 1996 Nuclear Data Symposium (JAERI-Conf 98-003, pp. 322-327, 1998) with the following abstract.

We perform intercomparison of delayed neutron activities calculated with JEF2.2, ENDF/B-VI and JNDC-V2 with a simple new method. Significant differences are found at $t < 20$ (s) for major fissioning systems. The differences are found to stem from fission yields or decay data of several nuclides. The list of these nuclides is also given for the future experimental determination of these nuclear data.

VII-A-9

Easy-to-use Application Programs for Decay Heat and Delayed Neutron Calculations on Personal Computers

K. Oyamatsu

A paper on this subject was published in Proc. 1996 Nuclear Data Symposium (JAERI-Conf 98-003, pp. 328-333, 1998) with the following abstract.

Application programs for personal computers are developed to calculate the decay heat power and delayed neutron activity from fission products. The main programs can be used in any computers from personal computers to main frames because their sources are written in Fortran. These programs have user friendly interfaces to be used easily not only for research activities but also for educational purposes.

VII-A-10

Consistency among Integral Measurements of Aggregate Decay Heat Power

H. Takeuchi, M. Sagisaka, K. Oyamatsu, Y. Kukita

A paper on this subject was published in Proc. 1996 Nuclear Data Symposium (JAERI-Conf 98-003, pp. 334-339, 1998) with the following abstract.

Persisting discrepancies between summation calculations and integral measurements force us to assume large uncertainties in the recommended decay heat power. In this paper we develop a hybrid method to calculate the decay heat power of a fissioing system from those of different fissioning systems. Then, this method is applied to examine consistency among measured decay heat powers of ^{232}Th, ^{233}U, ^{235}U, ^{238}U and ^{239}Pu at YAYOI. The consistency among the measured values are found to be satisfied for the β component and fairly well for the γ component, except for cooling times longer than 4000 s.

VIII. Osaka University

A. Department of Nuclear Engineering

VIII-A-1

Measurement of Double Differential Cross Sections of Charged Particle Emission Reactions for ^{27}Al and ^{nat}Ti by Incident DT Neutrons

Akito Takahashi, Hiroyuki Takagi, Kokooo and Isao Murata

Li_2ZrO_3, $LiAlO_2$ and Li_2TiO_3 can be considered to use as solid breeder material in fusion power reactors because of their inherent advantages, e.g., chemical stability at high temperature, compatibility with structural materials, good tritium recovery characteristics and so on. Thus, fusion neutronics experiments have been done for these materials at FNS of JAERI, Japan. In connecting with these experiments, double differential cross sections(DDXs) of ^{nat}Zr(n,xp) reaction induced by incident DT neutrons were measured at OKTAVIAN of Osaka University, Japan, in 1997 and the DDXs of ^{27}Al(n,xp), ^{27}Al(n,x α), ^{nat}Ti(n,xp) and ^{nat}Ti(n,x α) reactions have been measured in 1998. Experiments were carried out by using the charged particle spectrometer based on the E(CsI)-TOF two dimensional analysis of energy and time-of-flight of an emitted charged particle [1].

In the DDX and EDX data of ^{27}Al(n,xp) reaction, the present result agrees well with the measured data of Grimes's[2], JENDL-FF and SINCROS-II calculation. As shown in Fig.1, the measured data and evaluation for ^{27}Al(n,x α) reaction show good agreement with each other above 4.5MeV. However, overestimate of the JENDL-FF is shown below 4.5MeV. As for ^{nat}Ti(n,xp) reaction, the JENDL-FF and SINCROS-II were smaller than the measured EDX data above 7.5MeV. The measured DDX and EDX data for ^{nat}Ti(n,x α) reaction were not in agreement with JENDL-FF and SINCROS-II. The total charged particle emission cross sections for the present measurement are shown in Table 1.

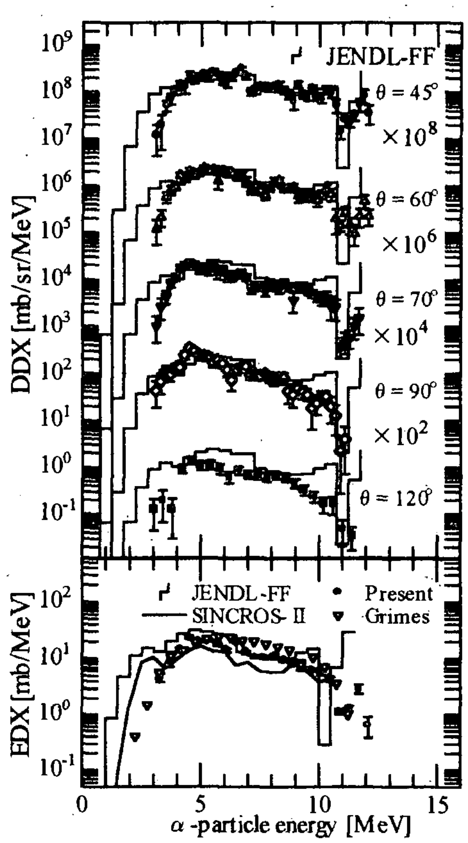

Fig. 1 The DDX and EDX data of Al(n,x α) reaction.

Table 1 The measured total charged particle emission cross-sections.

Reaction	Present Exp. σ(mb)	JENDL-FF σ(mb)	Other Exp. σ(mb)
^{27}Al(n,xp)	286.2±5.8	361.4	399±60 [2]
^{27}Al(n,x α)	91.3±1.5	125.2	121±25 [2] 143±7 [3]
^{nat}Ti(n,xp)	153.1±6.4	105.4	117.4 [2]
^{nat}Ti(n,x α)	34.8±1.2	39.5	36.1 [2]

References

[1] A.Takahashi, *et al.*, Nucl. Instr. Meth., A 401, 93 (1997).

[2] S.M.Grimes, *et al.*, Nucl. Sci. Eng., 62, 187 (1977).

[3] D.W.Kneff, et al., Nucl. Sci. Eng., 92, 491 (1986).

VIII-A-2

Measurements of ^{9}Be-d Nuclear Reaction Cross Sections at Low Energy

Akito Takahashi, Kimiya Ishii, Kentaro Ochiai, Isao Murata, Hiroyuki Miyamaru

A paper on this subject was presented at the 1998 Symposium on Nuclear Data, and published in JAERI-Conf., with the following abstract.

Differential cross section data of charged-particle emission from light elements with incident low energy protons/deuterons are useful for estimating dose-rate (PKA, KERMA) and material damage. Beryllium (^{9}Be) metal and ^{9}Be compound material are prospective candidates for the first wall materials of future fusion reactors. The use of neutral beam injector with several hundred keV and several amperes has been reported recently for inducing the temperature and density of plasma. To study plasma-particle/first-wall interaction problems on low energy nuclear reactions, we have measured charged-particle emission cross sections of ^{9}Be (d,x) and ^{9}Be (p,x) at low energy, where x = p, d , t and α, since, up to now the cross section data at low energy have not been obtained sufficiently. Especially, there are only few data of differential particle emission cross sections available for charged-particles produced by ^{9}Be (d,x) at low deuteron energy.

This work has used two accelerators. One is the Cockcroft-Walton type accelerator, OKTAVIAN at Osaka University, to measure the cross sections below 300 keV. The other is the tandem-Pelletron type accelerator, 5SDH-2 at Kobe University of Mercantile & Marine, to obtain the cross sections between 0.3 MeV and 1 MeV and to analyze the damage of beryllium samples after implanting beam. The samples were set up at the beam irradiation position by a manipulator with a stepping motor to obtain the flesh point on the sample for the beam implantation. Charged-particles emitted by ^{9}Be (d,x) reactions have been measured with two Si-Surface Barrier Detectors (Depletion layer: about 200μm). One detector could be moved between the angle from 30 degree to 160 degree for the measurement of angular-distributions of cross sections (differential cross sections). The other detector was fixed at 60 degree to make relative normalization for counts of particles detected at each angle. A Faraday-cup for beam-current monitor was set up at the backside of the beryllium sample. An aluminum thin foil was mount in front of the each SSBD for the screening of scattering deuteron.

As a result of our experiments, spectra data with peaks of (d,p), (d,t_0), (d,t_1), (d,α_0), (d,α_1) and (d,α_2) reactions with ^{9}Be target could be measured clearly and the differential cross sections of individual channel could be obtained below 1 MeV. Energy dependences of cross-sections for all reactions were reduced considering the Coulomb barrier transmission coefficient [1]. Also it was shown that angular distributions of cross sections for some reactions tended to be asymmetric around 90 degree (forward- or backward-peaking).

VIII-A-3

Benchmark Experiment on Cu, W, $LiAlO_2$ Assemblies with D-T Neutrons

—Leakage Neutron Spectrum Measurement—

A. Takahashi, T. Nishio, Kokooo, T. Kondo, H. Takagi,
I. Murata , F. Maekawa* and H. Takeuchi*

The benchmark experiments were carried out for Cu, W and $LiAlO_2$ at Fusion Neutronics Source (FNS) in JAERI, Japan. $LiAlO_2$ is regarded as an advanced solid breeder material and, Cu and W are the structural materials used in a fusion reactor. Leakage neutron spectra from the slab assemblies were measured using an NE-213 scintillation detector by the time-of-flight (TOF) method for two emission angles of 0 and 24.9 degree.(1) A high-energy-resolution measurement, ranging from 0.05 to 15 MeV, was achieved by the pulse-shape-discrimination technique with three delay–line amplifiers which were set to different gains.(2) The detector efficiencies were determined by using three measurements of a leakage neutron spectrum from beryllium assembly, energy and angle differential cross section of hydrogen using a polyethylene, neutron spectrum of ^{252}Cf spontaneous fission neutron source with the TOF method and SCINFUL calculation.(2)

The measured spectra were compared with the calculated results which were obtained by using the Monte Carlo code MCNP-4A in order to discuss the validation of the evaluated nuclear data files of JENDL-3.2, JENDL-fusion file, FENDL-1 and FENDL-2. The measured neutron angular flux spectrum compared with the calculation for $LiAlO_2$ assembly of 25 cm thickness at 0 degree angle point using JENDL-3.2 and JENDL-fusion file is shown in Fig.1. The measured data are in excellently good agreement with the evaluated nuclear data.

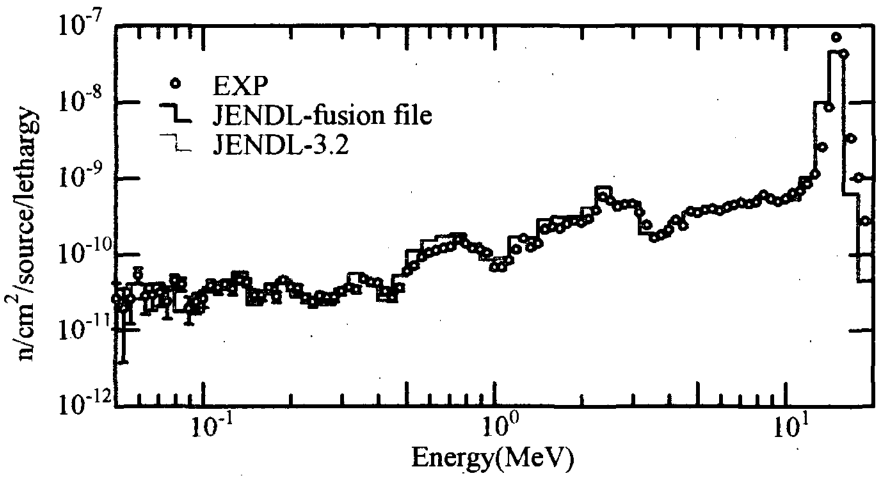

Fig. 1. Neutron flux for $LiAlO_2$ of 25 cm in thickness at 0 deg.

Reference:

(1) Kokooo, et al., "Benchmark Experiment on Vanadium Assembly with D-T Neutrons – Leakage Neutron Spectrum Measurement-", Proc. 1997 Symposium on Nuclear Data, Nov. 27-28, 1997, JAERI, Tokai, Japan, JAERI-Conf 98-003, pp. 204

(2) Kokooo, et al., Fusion Technol., 34, 980 (1998)

* High Energy Neutron Laboratory, Japan Atomic Energy Research Institute.

VIII-A-4

Measurement of Secondary Gamma-ray Production Cross Sections of Vanadium Induced by D-T Neutrons

Isao Murata, Tetsuo Kondo and Akito Takahashi

A paper on this subject presented at the 1998 Symposium on Nuclear Dada, Nov. 19-20, 1998, JAERI, Tokai, Japan with the following abstract:

1) Introduction

Vanadium has a potential to be used as a candidate structural material for the fusion reactor, because it has low activation property. At JAERI[1] and Osaka University, the data concerning this material have been obtained, for example, Kokooo et al. has measured the double differential cross sections of charged particle emission reaction induced by D-T neutrons[2]. In the present study, the measurement of secondary gamma-ray production cross sections of vanadium has been carried out. The theoretical calculations for the cross sections were done to compare with the measured data and other experimental results.

2) Experiment

The D-T neutron source OKTAVIAN at Osaka University was used. We adopted the TOF method to separate n-γ signals. Hp-Ge detector was used as gamma-ray detector. As the detector has high energy resolution, it is suitable for detailed gamma-ray measurements. The sample was natural vanadium the shape of which was a hollow cylinder (30mm-OD, 26mm-ID and 70mm in length). Using a thin sample, we could suppress neutron multiple scattering and attenuation of produced gamma-rays in the sample. The scattering angle was fixed at 125 deg. so that we didn't have to consider the angular distribution for secondary gamma-ray to estimate the total gamma-ray production cross section. The HP-Ge detector was shielded heavily by lead, heavy concrete, polyethylene, and so on. So we could suppress gamma-ray background and noise generated in the Ge crystal by fast neutrons.

3) Results and Discussion

Some corrections were considered as follows: Calculations of neutron multiple scattering and gamma-ray attenuation in the sample were done with MCNP-4a. Gamma-ray attenuation by air was corrected by absorption coefficient for air. The theoretical calculation for cross sections was made using SINCROS-Ⅱ. The experimental data was compared with the theoretical calculation results. And they were also compared with the cross section compiled data by Simakov et al.[3] which were evaluated with other experimental data.

References

[1] F. Maekawa et al. Fall Meeting of the Atomic Energy Society of Japan,A-11 (1997).
[2] Kokooo et al. Annual Meeting of the Atomic Energy Society of Japan,E-6 (1998).
[3] S.P. Simakov et al. private communication (1997).

B. Department of Chemistry

VIII-B-1

Sudden Changes in the Characteristics of GDR Fission of ^{238}U around the Critical Energy for Nuclear Phase Transition

Naruto Takahashi*, Akihiko Yokoyama*, Hiroshi Baba*, Takayuki Yamaguchi*, Daisaku Yano*, Tadashi Saito*, Noriko Nitani*, Yasunori Hamajima†, Tsutomu Ohtsuki‡, and Kazuyoshi Masumoto‡

A paper on this subject was published in Radiochimica Acta, Vol. 80, (1998) pp. 171-179 with the following abstract.

Abstract:

Photofission of ^{238}U with the bremsstrahlung of the end-point energies, 15, 30, and 60 MeV was studied radiochemically to elucidate the characteristics of the fission of ^{238}U nucleus excited via the giant dipole resonance (GDR) in contrast to those in the lower energy region. Observed charge dispersion widths for 30- and 60-MeV bremsstrahlungs were broad, just as those found among various types of energetic particle-induced fission, while the width for the 15-MeV case turned out to be equal to that reported for thermal neutron fission. The obtained charge and mass-yield distributions also revealed distinct differences between the above two groups; one characteristic of fission at moderate excitation and the other of low-energy fission. The average excitation energy was calculated from the spectrum of bremsstrahlung and the fission cross section was found to locate within the GDR region in all cases. The analysis of the peak-to-valley ratio revealed that the fission takes place without the emission of the pre-fission neutrons. It was pointed out that this sudden change of the fission characteristics took place around the critical energy for nuclear phase transition.

*Department of Chemistry, Graduate School of Science, Osaka University
†Department of Chemistry, Faculty of Science, Kanazawa University
‡Laboratory of Nuclear Science, Faculty of Science, Tohoku University

VIII-B-2

Fast Fission Mechanisms in the Carbon-Induced Fission of Uranium

Akihiko Yokoyama*, Hiroshi Baba*, Naruto Takahashi*, and Tadashi Saito*

A paper on this subject was published in Journal of Alloys and Compounds, Vol. 271-273, (1998) pp. 322-326 with the following abstract.

Abstract:

The conventional radiochemical technique was applied to the ^{12}C-induced fission of ^{238}U at incident energies below and above the borderline for the appearance of fast fission. It supplies information on the charge dispersion and distribution of fission products in addition to the mass distribution for isolation of fast fission from ordinary fusion fission. The resulted width of charge dispersion was independent of A except for the case of the 140-MeV incident energy, where the widths at far-asymmetric mass region were definitely large compared to the normal value. On the other hand, the observed variances of mass distribution change around the threshold energy for fast fission more drastically than prediction by the model assuming that they are controlled by the stiffness coefficient and the temperature. We conclude that both results suggest the appearance of far-asymmetric mass distribution associated with the set-in of fast fission .

*Department of Chemistry, Graduate School of Science, Osaka University

VIII-B-3

Determination of Formation Cross Section by γ Spectrometry: Derivation of Universal Correction formulas for Ingrowth during Irradiation

Hiroshi Baba*, Jun Sanada*, Hirokazu Araki*, and Akihiko Yokoyama*

A paper on this subject was published in Nuclear Instruments and Methods in Physics Research A, Vol. 416, (1998) pp. 301-313 with the following abstract.

Abstract:

We have derived generalized correction formulas for the effect of ingrowth from the precursor during irradiation in the determination of the formation cross section by γ spectrometry. The correction formulas enabled one to carry out the correction quite easily. They require no detailed decay schemes of involved nuclides , except for the half-lives and, in case where nuclear isomers exist, the fraction of transition between any pair of the nuclides, and thus make it possible to get rid of tedious derivation of individual correction formulas . The whole procedure is easily programmed in a personal computer and one can instantaneously judge whether a correction is necessary for a relevant nuclide. Further, it supplies correction factors to deduce both the independent and cumulative yields of a nuclide from the extrapolated yield to the end-of-bombardment(EOB) in the decay analysis on one hand and also those to be applied to the chemically separated activities at EOB. The latter set of correction factors are applicable to physically separated activities in ISOL or gas-jet transport experiments as well, provided that the effective retention duration of the product nuclides in the reaction chamber is known.

*Department of Chemistry, Graduate School of Science, Osaka University

VIII-B-4

Fast Fission Mechanism and Duality of the Diffusion Process

Hiroshi Baba*, Naruto Takahashi*, Akihiko Yokoyama*, and Tadashi Saito*

A paper on this subject was published in the European Physical Journal A, Vol. 3, (1998) pp. 281-292 with the following abstract.

Abstract:

The reaction of ^{238}U with ^{12}C was studied radiochemically with the purpose of elucidating fast fission characteristics. From the difference in the mass distribution below and above the critical energy where fast fission is predicted to set in, fast fission component was extracted in far-asymmetric mass region and interpreted as the mass diffusion following the Fokker-Planck equation. Anomalous charge dispersion widths in the corresponding mass region and a sudden increase of the whole mass distribution width at the critical energy were also observed to support the above result. The reaction time of fast fission deduced from the width and position of the mass distribution was 5×10^{-21}s as well by taking into account the effect of neutron emission during the diffusion process, which turned out to be more than one order of magnitude longer than the corresponding life time of typical deep inelastic scattering but substantially short compared to ordinary fusion-fission life time. Evaluation of the driving potential for mass drift required dinuclear configuration be of an elongated or deformed form for fast fission in contrast to a more compact form for the deep-inelastic process.

*Department of Chemistry, Graduate School of Science, Osaka University

IX. Tohoku University

A. Department of Quantum Science and Energy Engineering

IX-A-1

Measurements of Double-Differential Neutron Emission Cross Sections of ^{6}Li, ^{7}Li and ^{9}Be for 11.5 MeV and 18.0 MeV Neutrons

Masanobu Ibaraki, Mamoru Baba, Shigeo Matsuyama, Toshiya Sanami, Than Win, Takako Miura and Naohiro Hirakawa

A paper of the title was published in J. Nucl. Sci. Technol., Vol.35, No.12, (Dec. 1998) pp.843-850 with the following abstract.

Double-differential neutron emission cross sections (DDXs) of ^{6}Li, ^{7}Li and ^{9}Be were measured for 18.0 MeV and 11.5 MeV incident neutrons produced by the T(d,n) and $^{15}N(d,n)$ reactions respectively, using the Tohoku University Dynamitron time-of-flight (TOF) spectrometer. The data were obtained at 13 laboratory angles, and angular-differential cross sections (ADXs) of elastic and inelastic scattering neutrons were derived from the DDXs. For 11.5 MeV neutrons, we obtained the neutron emission spectra over the secondary neutron energies by newly employing the double TOF method as well as the conventional one. In the measurements at 18.0 MeV, we achieved better energy resolution than in our previous studies by using a neutron detector that has a larger solid angle and a thinner tritium target. The experimental results of DDXs and ADXs were compared with our previous results and the evaluated data given in JENDL-3.2, JENDL Fusion File and ENDF/B-VI. It is found that the JENDL data reproduce the experimental ones very well.

IX-A-2

High resolution measurements of double differential (n,α) cross sections of ^{58}Ni and ^{nat}Ni between 4.2 and 6.5 MeV neutrons

Toshiya Sanami, Mamoru Baba, Toshihiko Kawano[1], Shigeo Matsuyama, Takehide Kiyosumi, Yasushi Nauchi, Keiichiro Saito, Naohiro Hirakawa

A paper of the title was published in J. Nucl. Sci. Technol., Vol.35, No.12, (Dec. 1998) pp.850-856 with the following abstract.

Double differential (n,α) reaction cross sections of ^{58}Ni and ^{nat}Ni were measured for 4.2~6.5MeV neutrons with energy resolution good enough to separate α particles from the low-lying levels of residual nuclei by using a gridded ionization chamber. Angular distribution and excitation functions were derived for α_0, α_1 and $\alpha_{i\geq 2}$ components (α-particles to the ground level, the 1st level and levels higher than the 2nd level, respectively).

The experimental results were compared with these obtained from calculation based on Hauser-Feshbach model employing the optical potential and the level density parameters derived to reproduce the experimental values of total, (n,p) and (n,α) cross sections. The calculation showed fair agreement with the experimental data while it underestimated the (n,α) cross section above 6 MeV.

----

1. Advanced Energy Engineering Science, Kyushu University

IX-A-3

Measurements of (n,xp), (n,xd) Double Differential Cross Sections of Carbon and Aluminum for 65 and 75MeV Neutrons

Yasushi Nauchi, Mamoru Baba, Toshiya Sanami, Masanobu Ibaraki, Tomohiko Iwasaki, Naohiro Hirakawa, Susumu Tanaka, Shin-ichiro Meigo, Hiroshi Nakashima, Hiroshi Takada, Takashi Nakamura, Yukinobu Watanabe

A paper of the title was published in J. Nucl. Sci. Technol., Vol.36, No.1, (Jan. 1999) with the following abstract.

Double differential (n,xp), (n,xd) cross sections of carbon and aluminum were measured for 65 and 75MeV neutrons at angles between 12deg and 70deg using ΔE-E telescopes at a ^{7}Li(p,n) neutron source facility at TIARA.

The data at 12deg were obtained by employing an annular geometry. The telescopes consisting of SSD and NaI(Tl) scintillator, experimental methods and the data reduction procedures are presented as well as the results. The carbon data are compared favorably with existing experimental data.

The (n,xp) spectra of both carbon and aluminum agreed fairly well with theoretical calculations based on the intra-nuclear cascade model and the multi-step Hauser-Feshbach model including pre-equilibrium effects, but the (n,xd) spectra differ significantly from those calculations.

IX-A-4

Double-differential Neutron Emission Cross Section for 11.5 and 18.0 MeV Neutrons

M. Baba, S. Matsuyama, M. Ibaraki, D. Soda, T. Ohkubo, T. Sanami, Than Win, T. Miura, N. Hirakawa

A paper of the title was published in the Proc. Int. Conf. on Nucl. Data for Sci. & Technol., (Trieste 1997), pp. 535-537 with the following abstract.

Double-differential neutron emission cross sections for 11.5 and 18 MeV Neutrons have been measured down to ~ 1 MeV secondary energies with an improved energy resolution. The measurements at 11.5 MeV were realized by using the ^{15}N(d,n) source and "double-TOF" method, and the energy resolution of the spectrometer was improved by use of a long liquid scintillation detector.

IX-A-5

Measurements of Double-differential Neutron Emission Cross Sections of ^{6}Li, ^{7}Li and ^{9}Be for 18 MeV Neutrons

M. Ibaraki, M. Baba, S. Matsuyama, T. Sanami, Than Win, T. Miura, N. Hirakawa

A paper of the title was published in the Proc. Int. Conf. on Nucl. Data for Sci. & Technol., (Trieste 1997), pp.610-612 with the following abstract.

Double-differential neutron emission cross sections of ^{6}Li, ^{7}Li and ^{9}Be for 18 MeV neutrons were measured with an improved energy resolution than that in our previous study. Experimental results were compared with the evaluated data and, for ^{9}Be, also with a simple model calculation.

IX-A-6

Measurements of (n,xp), (n,xd) double differential cross sections of Al and C for Ten's MeV Neutrons

Y. Nauchi, M. Baba, T. Sanami, T. Iwasaki, N. Hirakawa,
T. Nakamura, S. Tanaka, S. Meigo, Y. Watanabe, M. Harada, H. Takada

A paper of the title was published in the Proc. Int. Conf. on Nucl. Data for Sci. & Technol. (Trieste 1997), pp.613-615 with the following abstract.

Double Differential (n,xp) and (n,xd) cross sections of carbon and aluminum were measured for 64 and 75MeV neutrons between 12deg and 70deg. These (n,xp) data are compared favorably with a modified version of cascade model code, ISOBAR, taking account of in-medium NN cross sections and Q-value of (p,n) and (n,p) reactions.

IX-A-7

Measurements of (n,xα) Cross Section Using Gaseous Sample and Gridded Ionization Chamber

T.Sanami, M.Baba, K.Saito, Y.Ibara, N.Hirakawa

A paper of the title was published in the Proc. Int. Conf. on Nucl. Data for Sci. & Technol., (Trieste 1997), pp.616- 618 with the following abstract.

We developed a method of (n,α) cross section measurement using a gaseous sample in a gridded ionization chamber. This method enables to measure the cross section with large solid angle without the distortion by the energy loss in the sample. We developed a method to determine the detection efficiency which has been difficult to estimate for gaseous samples by using GIC signals and tight neutron collimation. The method is applied to the $^{16}O(n,\alpha)$ cross section measurement around 14 MeV.

B. Laboratory of Nuclear Science

IX-B-1

Measurement of the ^{6}Li(e,e′p) reaction cross sections at low momentum transfer

T. Hotta, T. Tamae, T. Miura, H. Miyase[1], I. Nakagawa, T. Suda[1], M. Sugawara, T. Tadokoro A. Takahashi, E. Tanaka and H. Tsubota[1]

A paper on this subject will be published in Nuclear Physics with the following abstract:

The triple differential cross sections for the ^{6}Li(e,e′p) reaction have been measured in the excitation energy from 27 MeV to 46 MeV to search for evidences of the giant dipole resonance (GDR) in ^{6}Li. The cross sections have no distinct structures in this energy region, and decrease smoothly with the energy transfer. Angular distributions are different from those expected with the GDR. Protons are emitted strongly to the momentum-transfer direction. The data are well reproduced by a DWBA calculation assuming a direct proton knockout process.

[1]Physics Department, Graduate School of Science, Tohoku Univ.

IX-B-2

Study of the giant resonance of ^{40}Ca by the (e,e′n) reaction

K. Yoshida[1], T. Saito, M. Oikawa[2], T. Endo[3], K. Kino, K. Takahashi, T. Nakagawa[3], K. Abe[4] and H. Ueno[5]

The cross sections and angular correlations for the ^{40}Ca(e,e′n) reaction have been measured in the excitation energy range just above the giant dipole resonance, at the effective momentum transfer of 0.35fm^{-1}. In the previous ^{40}Ca(e,e′n) experiment[1)], it was found that neutron decay of the E1 giant resonance leads predominantly to the ground and first excited states and the cross sections for these neutrons decrease rapidly with increasing the excitation energy. On the other hand, Murakami et al.[2)] have pointed out the existence of the isovector E2 giant resonance around 30 MeV from the angular asymmetry measurement of the neutron for the ^{40}Ca(γ,n) reaction.

The experiment was performed using the continuous electron beam from the 150-MeV Tohoku University pulse stretcher ring. A natural calcium target of thickness 107 mg/cm^2 was bombarded with electron of energy 126 MeV. The scattered electrons were detected at $\theta_e = 30°$ by a magnetic spectrometer and the emitted neutrons were detected using ten NE213 liquid scintillator neutron detectors.

The angular correlations have been measured in energy range 28-35 MeV at ten points $\theta_n = 50°$ to $\theta_n = 270°$. Figure 1 shows a missing energy spectrum summing up all data at $\theta_n = 70°$. No peaks were found at 15.6 and 18.7 MeV which correspond to the ground and first excited state transitions observed in the previous experiment. A observed broad peak around 20 MeV indicates that neutron decays from the region above giant dipole resonance feed mostly to the excited states of about 5 MeV.

Figure 2 shows the angular coefficients obtained by Legendre polynomials expansion for the angular correlations measured. The coefficients are compared with those for the n_1 group in the previous experiment. Both data are connected together smoothly besides the b_2 parameter. The parameters b_1 and b_3 are not zero, which suggests an E2 component in this energy region. A large value of c_2 at 29 and 30 MeV might be due to systematic error. The transverse-transverse interference term d_2 is very small as expected.

[1] Toshiba Co.
[2] Japan Defense Agency
[3] Department of Pysics, Tohoku Univ.
[4] Department of Nuclear Engineering, Tohoku Univ.
[5] Department of Physics, Yamagata Univ.

Figure 3 shows the cross sections together with the previous (e,e′n) measurement and (γ,n) cross sections. The present cross sections are connected with previous ones and show a little bit larger cross section than the (γ,n) ones.

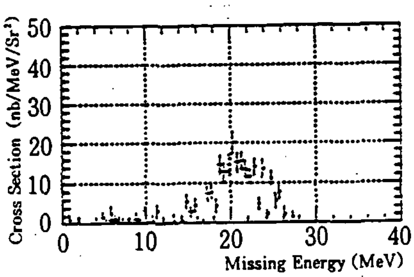

Fig.1 Missing energy spectrum for the ^{40}Ca(e,e′n) reaction.

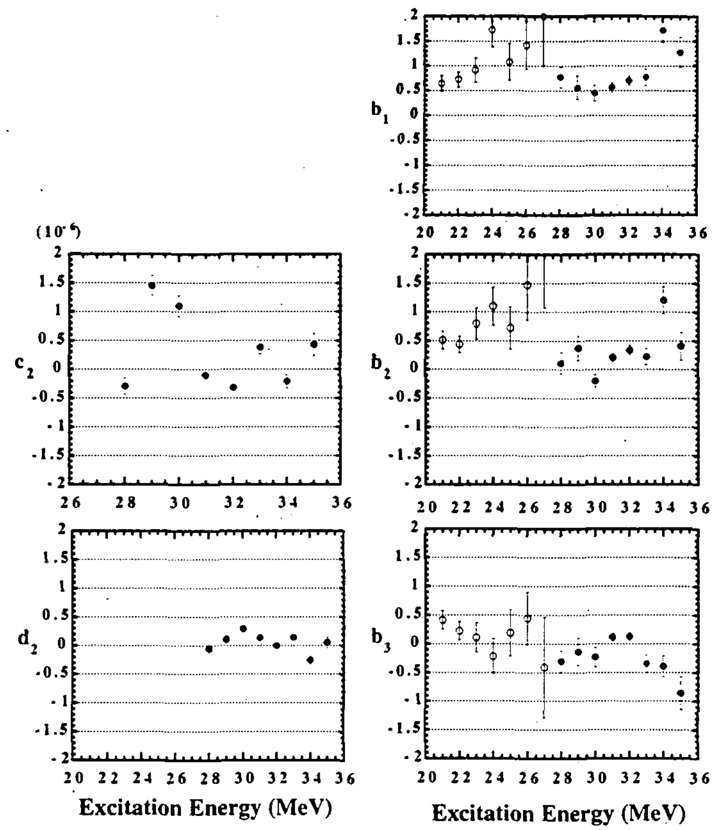

Fig.2 The angular coefficients obtained by a fit of the Legendre polynomials.

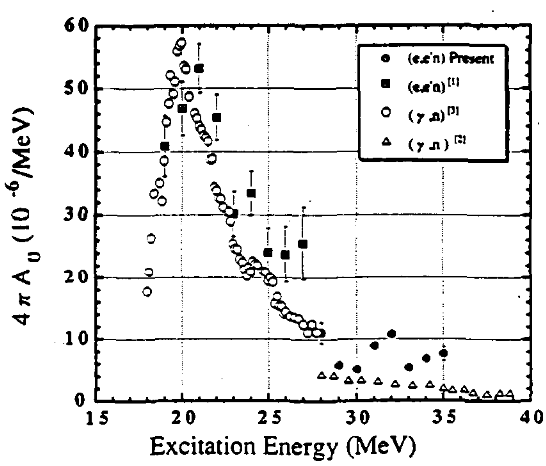

Fig.3 Comparison between the ^{40}Ca(e,e′n) and ^{40}Ca(γ,n) cross sections. ^{40}Ca(e,e′n) (present) : closed circles, ^{40}Ca(e,e′n) (ref.1) : closed squares, ^{40}Ca(γ,n) (ref. 2) open triangles, ^{40}Ca(γ,n) (ref. 3) : open circles.

References:

1) C. Takakuwa, T. Saito, S. Suzuki, K. Takahisa, T. Tohei, T. Nakagawa and K. Abe: Phys. Rev.C46 (1992) 1880.
2) T. Murakami et al.: J. Phys. G14 (1988) S275.
3) J. Kellie, A.R. Curran, S.J. Hall, G.I. Crawford, J.L. Robertson and D.T. Burns: Nucl. Phys. A515 (1990) 125.

C. Cyclotron and Radioisotope Center

IX-C-1

Measurement of induced radioactivity in copper exposed to high energy heavy ion beam

Eunjoo KIM, Takashi NAKAMURA, Yoshimoto UWAMINO, Sachiko ITO, Akifumi FUKUMURA

The residual radioactivities produced by high energy heavy ions have been measured using the heavy ion beams of the Heavy Ion Medical Accelerator (HIMAC) at National Institute of Radiological Sciences. The spatial distribution of residual radioactivities in 3.5cm, 5.5cm and 10cm thick copper targets of 10cm×10cm size bombarded by 290MeV/u, 400MeV/u-^{12}C ion beams and 400MeV/u-^{20}Ne ion beam, respectively, were obtained by measuring the gamma-ray activities of 0.5mm thick copper foil inserted in the target with a high purity Ge detector after about 1hour to 6 hours irradiation.

1. Introduction

In radiation safety design of high energy and high intensity accelerator, the evaluation of residual radioactivities of accelerator and shielding materials is very important for protection of radiation workers, especially during maintenance work. The radioactivities of air, coolant water and soil are also important for protection of natural environment and nearly inhabitants. The residual radioactivities are produced by accelerating charged particles and secondary neutrons. Those by charged particles are a main source in accelerator materials exposed to a beam. Nevertheless, there exist very few experimental data of residual radioactivities produced by high energy heavy ions and the accurate estimation method has not been established yet. Several experimental studies on the reaction between carbon ion beam and copper target have been reported at projectile energies of 15 to 90MeV/u [1-3]. In this study, we performed irradiation experiments of copper target using the 290MeV/u and 400MeV/u ^{12}C ions and 400MeV/u ^{20}Ne ion beams of the Heavy Ion Medical Accelerator in Chiba (HIMAC) at National Institute of Radiological Sciences.

2. Experiments

Irradiation was performed with 290 and 400MeV/u-^{12}C ion beams , and 400MeV/u-^{20}Ne ion beam delivered from HIMAC. Figure 1 shows an assembly of the natural copper target of 10cm×10cm size and 0.5cm thickness which has total thickness of copper target of 3.5cm, 5.5cm and 10cm to stop the projectile heavy ion beams, 290 and 400MeV/u-^{12}C ion beam and 400MeV/u-^{20}Ne ion beam, respectively. Additional copper activation foils of 10cm×10cm and 0.5mm thickness were inserted at every 5mm to 20mm interval in the copper target to measure the spatial distribution of residual radioactivities in the copper target.

The size of projectile beam is about 1cm in diameter and the beam perpendicularly bombarded the target. The irradiation condition and the activation foils used in the experiment are listed in Table1. During irradiation experiment, the beam intensities were measured with an transmission-type ionization chamber .

The gamma rays from residual radioactivities in copper foil inserted in the copper target were measured by the high purity Ge detector by coupling with the 4096 multi-channel analyzer. The measuring time of copper foils was between 60min and 5hours, and the cooling time was between 6min and 5days from beam off, considering the half lives of residual radioactive nuclides. From the measured gamma-ray spectra , we identified a number of radionuclides and the reaction rate of residual nuclei were obtained from the peak counts after corrected with the peak efficiency of Ge detector

3. Results and Discussion

From the irradiation experiments, we identified the residual nuclei of these activation foils and obtained the spatial distribution of their reaction rates in the copper target. Table2 gives the measured residual nuclides in copper activation foil. The number of identified radionuclides is 14, 17, 19 and 39, the mass number of residual nuclides is between 27(^{27}Mg) and 61(^{61}Cu) for 290MeV/u ^{12}C ion bombardment during 1hour irradiation time, 24(^{24}Na) and 61(^{61}Cu) for 400MeV/u ^{12}C ion bombardment during 1hour irradiation time, 27(^{27}Al) and 63(^{63}Zn) for 400MeV/u ^{20}Ne ion bombardment during 1hour irradiation time, 7(^{7}Be) and 63(^{63}Zn) and for 400MeV/u ^{12}C ion bombardment during 6 hours irradiation time, respectively.

Table 2 Residual nuclides measured in the copper activation foil

Projectile heavy ion beam	Residual nuclides in copper activation foil
290MeV/u ^{12}C ion- ^{nat}Cu	^{27}Mg, ^{29}Al, ^{34m}Cl, ^{38}Cl, ^{39}Cl, ^{41}Ar, ^{44}Sc, ^{49}Cr, ^{56}Mn, ^{53}Fe, ^{61}Co, ^{62m}Co, ^{60}Cu, ^{61}Cu (14)
400MeV/u ^{12}C ion- ^{nat}Cu	^{24}Na, ^{29}Al, ^{34m}Cl, ^{38}Cl, ^{39}Cl, ^{40}Cl, ^{41}Ar, ^{43}Sc, ^{44}Sc, ^{49}Cr, ^{52m}Mn, ^{56}Mn, ^{53}Fe, ^{61}Co, ^{62m}Co, ^{60}Cu, ^{61}Cu (17)
400MeV/u ^{20}Ne ion- ^{nat}Cu	^{24}Na, ^{29}Al, ^{38}Cl, ^{40}Cl, ^{41}Ar, ^{43}Sc, ^{44}Sc, ^{44m}Sc, ^{49}Cr, ^{52m}Mn, ^{56}Mn, ^{53}Fe, ^{61}Co, ^{62m}Co, ^{60}Cu, ^{61}Cu, ^{56}Ni, ^{65}Ni, ^{63}Zn (19)
400MeV/u ^{12}C ion- ^{nat}Cu	^{7}Be, ^{24}Na, ^{28}Mg, ^{29}Al, ^{34m}Cl, ^{38}Cl, ^{39}Cl, ^{41}Ar, ^{42}K, ^{43}K, ^{44}K, ^{43}Sc, ^{44m}Sc, ^{44}Sc, ^{46}Sc, ^{47}Sc, ^{48}Sc, ^{48}V, ^{48}Cr, ^{49}Cr, ^{51}Cr, ^{52}Mn, ^{54}Mn, ^{56}Mn, ^{52}Fe, ^{59}Fe, ^{55}Co, ^{56}Co, ^{57}Co, ^{58}Co, ^{61}Co, ^{62m}Co, ^{60}Cu, ^{61}Cu, ^{56}Ni, ^{57}Ni, ^{65}Ni, ^{62}Zn, ^{63}Zn (39)

Figures 2 to 5 show the spatial distributions of ^{61}Cu, ^{56}Mn, ^{44}Sc and ^{38}Cl in the copper target for 290 and 400MeV/u ^{12}C ion and 400MeV/u ^{20}Ne ion bombardments.
Figures 2 and 3 show the spatial distributions of ^{61}Cu and ^{56}Mn in the copper target for 290 and 400MeV/u ^{12}C ion and 400MeV/u ^{20}Ne ion bombardments. These figures indicate that the spatial distributions of activation rates of ^{61}Cu and ^{56}Mn which are close to the target nucleus of natural Cu (^{63}Cu and ^{65}Cu) increase with penetrating the copper target, while on the other hand, the spatial distributions of ^{44}Sc and ^{38}Cl which have much smaller atomic number and mass number than natural Cu have a constant distribution in the copper target and steeply decrease at the point of energy range of the incident beam (2.5cm for 290MeV/nucleon ^{12}C , 4.0cm for 400MeV/u- ^{12}C and 2.5cm for 400MeV/u-^{20}Ne). It is also clear from Figs.2 to 5 that the spatial distributions of ^{61}Cu, ^{56}Mn, ^{44}Sc and ^{38}Cl which were produced by the 290 and 400MeV/u-^{12}C ions give similar activation rate curves with depth each other and steeply decrease at the stopping range of an incident beam, especially for ^{44}Sc and ^{38}Cl activation rates. We can find that the ^{61}Cu and ^{56}Mn spatial distributions extend in the copper target beyond the energy range of an incident beam, especially for 400MeV/u-^{12}C and ^{20}Ne ion incidences. This may be explained from the phenomenological fact that the ^{61}Cu and ^{56}Mn isotopes were mainly produced through ^{nat}Cu (n,xn) and (p,px) reactions by the secondary fragment particles, such as protons and neutrons, produced by ^{12}C interaction with copper, in addition to that by the direct reactions of an incident beam. On the other hand, ^{44}Sc and ^{38}Cl isotope productions have rather high threshold energy and were mainly produced by the direct reactions of ^{12}C and ^{20}Ne ion beams with copper target.

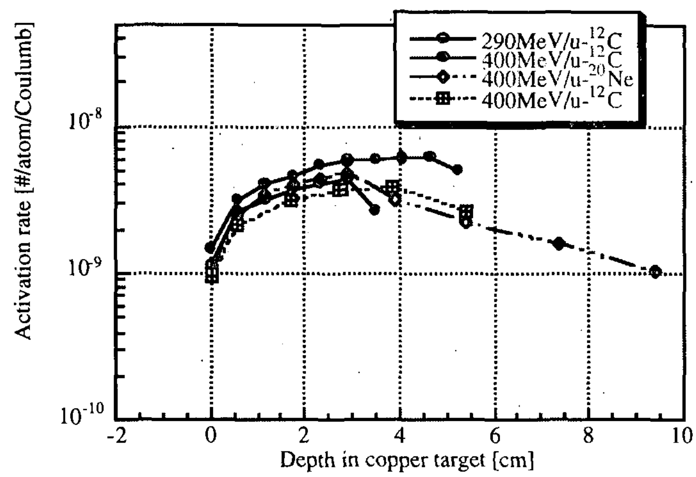

Fig.2 Spatial distribution of ^{61}Cu activation rate in the copper target

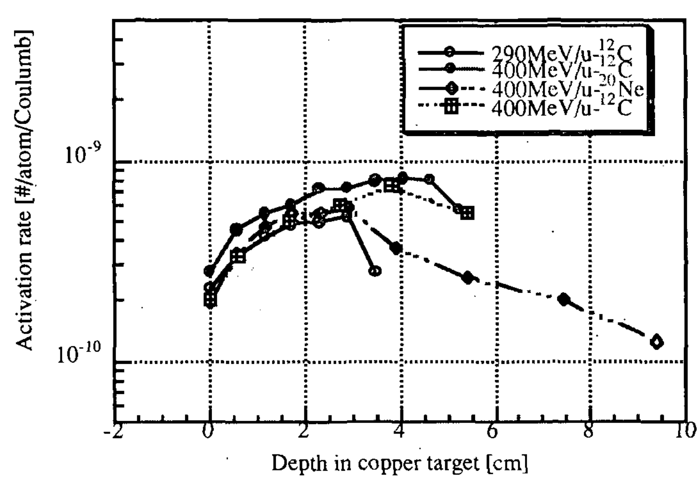

Fig.3 Spatial distribution of ^{56}Mn activation rate in the copper target

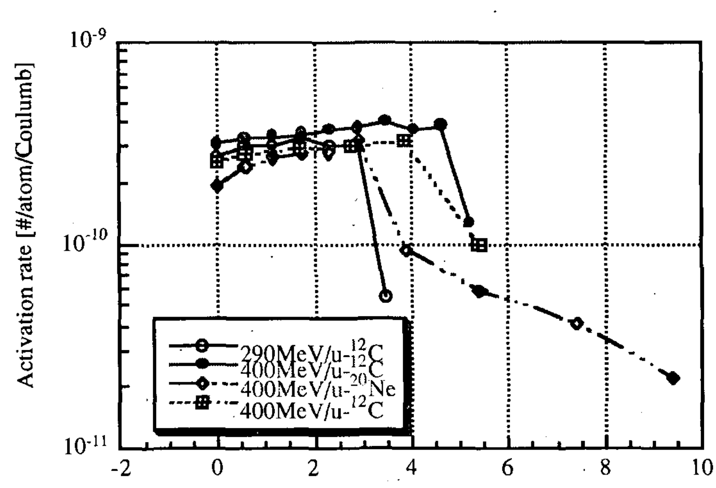

Fig.4 Spatial distribution of ^{44}Sc activation rate in the copper target

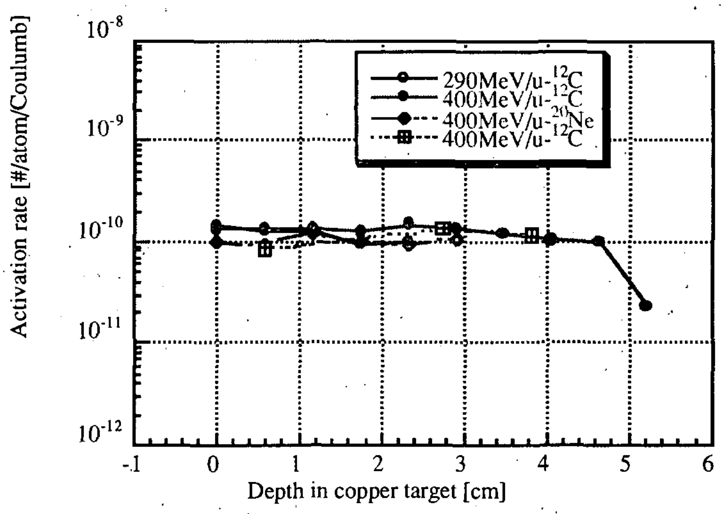

Fig.5 Spatial distribution of ^{38}Cl activation rate in the copper target

Acknowledgments
This work has been done as a Research Projectile with Heavy Ions at NIRS-HIMAC (National Institute of Radiological Sciences).

References

[1]Whitfield. J.P., Porile.N.T. : Phys. Rev. C47, 1636 (1993)
[2]Land T., Kolzahan D., Bergersen B., Hagebo E., Haldorsen I.R., Richared-Serre C.,: Z.Phys,A306,43(1982).
[3]Li Wenxin , Sun Tongyu, Wu Dingqing, Sun Rulin.: Radiochimaca Acta 72, 109 (1996)
[4]Annals of the ICRP, ICRP publication 51. (1987)

IX-C-2

Measurements of secondary particles produced from thick targets bombarded by heavy ions

Tadahiro KUROSAWA, Takashi NAKAMURA, Noriaki NAKAO
Tokushi SHIBATA, Yoshitomo UWAMINO, Akifumi FUKUMURA

We measured angular and energy distributions of neutrons, protons, deuterons and tritons produced by 100 MeV/nucleon He ions stopping in thick carbon, aluminum, copper and lead targets using the HIMAC (Heavy Ion Medical Accelerator in Chiba) of NIRS (National Institute of Radiological Sciences), Japan by using the time-of-flight method coupled with the ΔE-E counter system. The experimental spectra were compared with the calculation using the LCS code and the calculated spectra are generally in rather good agreement with the measured spectra of these four secondary particles.

1. INTRODUCTION

With the increasing use of high energy (higher than 100MeV/nucleon) heavy ions (heavier than He ion) in various fields, the energy-angle distribution of neutrons produced from a thick target which fully stops heavy ions becomes very important as the source-term data of shielding design of the accelerator facility. Although only one paper has ever been published on thick target neutron yield (TTY) for 177MeV/nucleon He ions [1], Heilbronn et al. [2] and our group [3, 4] have recently performed the experiments on TTY for 155MeV/nucleon He ions [2] and for 100, 180 MeV/nucleon He and 100, 180, 400MeV/nucleon C ions [3] , and for 100, 180, 400MeV/nucleon Ne ions [4]. In this work we present the angular - energy distributions of neutrons, protons, deuterons and tritons produced from thick carbon, aluminum, copper and lead targets bombarded by 100 MeV/nucleon helium ion. The charged particle spectra from thick targets are not so important in physical meaning due to the energy loss in the target depending on the target thickness, but these results will be useful as benchmark experimental data to investigate the accuracy of the particle-transport calculation code. Here, the measured spectra are compared with those calculated with the LAHET Code System, LCS [5] as a benchmark test.

2. EXPERIMENTAL PROCEDURE

The energy of neutrons, protons, deuterons and tritons produced in the target was measured by the time-of-flight (TOF) method. A thin NE102A plastic scintillator (3cm diam. by 0.05cm thick) was placed just behind the end window of the beam line as a beam pick-up scintillator. The output pulses of this scintillator were used as start signals of the TOF measurement, and also to count the absolute number of projectiles incident on the target. A target was set on the beam line 10 cm behind the beam pick-up scintillator. The beam spot size incident on the target was about 1.5 cm diameter and the beam height was 1.25m above the concrete floor of the experimental area. The NE213 liquid scintillator (12.7cm diam. by 12.7cm thick), which was designed to expand the dynamic range of output pulses for high energy neutron measurements[6], was used for neutron detector (E counter), and the NE102A plastic scintillator (15 cm by 15cm square and 0.5cm thick) for the ΔE counter was placed in front of the E counter to discriminate charged particles from noncharged particles, neutrons and photons. Three sets of E and ΔE counters were used for simultaneous angular distribution measurements at three different angles. The detectors were located 2 m at large angles to 5 m at small angles away from the target to provide better energy resolutions in the forward directions where there are larger yields of high energy neutrons. In order to minimize neutrons in scattering, no local shielding was used near the detectors. By interposing an iron shadow bar of 15cm by 15cm square and 60cm thickness between the target and detector, the background neutron components from room scattering were measured particularly at large angle. Target thicknesses were selected to stop the incident particles completely. Target materials are C (1.77g/cm^3), Al (2.7g/cm^3), Cu (8.93g/cm^3) and Pb (11.34g/cm^3) and each target has a shape of 10cm by 10cm square. The C, Al, Cu and Pb targets are 5.0, 4.0, 1.5 and 1.5 cm thick, respectively.

3. DATA ANALYSIS

3.1 Neutrons

As the ΔE counter does not scintillate by neutrons and gamma rays, the neutron and gamma ray events could be selected from the charged particle events, by using two-dimensional ΔE-E graphical plots. After this discrimination, the neutron and the gamma ray events were clearly separated by using two-dimensional graphical plots of total-slow pulse height components of the E counter. In this discrimination, the pulse shapes from high energy neutron events in which recoil protons escape from the E counter are close to those from gamma-ray events, and these events were eliminated from the neutron events. After each experimental run, each E counter was calibrated with a ^{60}Co gamma-ray source, and the Compton edge in the gamma-ray spectrum was used as the bias point of 1.25MeVee (electron equivalent) which corresponded to 3 MeV neutron energy. After obtaining the TOF spectrum of neutrons, the data were converted into the energy spectrum of neutrons. For this conversion, the detection efficiency of the NE213 E counter is essential. The experimental data of the detection efficiency for this scintillator has been published by Nakao et al.[6], but there is no data for neutrons of energy higher than 135MeV. Therefore, the neutron detection efficiency was calculated with the Monte Carlo code by Cecil et al.[7] for all energy range. Corresponding to the elimination of high energy neutron events as described above, the recoil proton events escaped from the E counter were also excluded from these calculated efficiencies.

3.2 Charged particles

To separate proton, deuteron and triton events, three kinds of two dimensional graphical plots were used. Two dimensional ΔE-E graphical plots were first used to identify different Z number particles, but this plots could not identify different mass number particles. In the two dimensional plots of TOF-E pulse height distributions for Z=1 particles, different mass particles of protons (m=1) deuterons (m=2) and tritons (m=3) are clearly separated, but the pulse heights of high energy particles escaped from the E counter intersect between those of different mass particles. This intersection was resolved in the following way. It is well known that slow components from the NE213 scintillator increase with increasing the specific energy loss (dE/dx) for a given type of charged particle. The charged particles escaped from the detector, which have the longer stopping range than the detector size, give small dE/dx values compared with the charged particles stopped in the detector and then slow components of the light outputs from escaped particles approach to the pulse heights of gamma rays. These results are shown in the two dimensional total-slow pulse height plots. The proton, deuteron and alpha particles have three separate lines in the order of dE/dx values of these three particles and the charged particles escaped from the detector are in the uppermost line independent to the particle mass. We first selected proton events by setting the region of interest (ROI) which included the events of escaped deuterons and tritons, and then eliminated the latter events by identifying the escaped particle events. This procedure was repeated for deuterons and tritons in this order. We finally obtained the TOF spectra for protons, deuterons and tritons separately. The TOF spectra were then converted to the energy spectra by approximating 100% detection efficiency of the NE213 detector.

4. MONTE CALRO SIMULATIONS

These experimental results were compared with the calculations as a benchmark test. The secondary particle spectra were calculated by using the LAHET Monte Carlo Code System, LCS[5]. The LCS calculations were performed for 100MeV/nucleon He incidence on stopping-length C, Al, Cu and Pb targets to investigate the calculational accuracy. The majority of the LAHET parameters was set to their default settings. The target dimension was fixed to be the same size as used in the experiment. The target was set at the center of the vacuum sphere and a total number of 200,000 He particles were injected normally to the target in the central circular surface of 0.5 cm diameter which simulated the actual beam geometry. The angular flux of particles of neutrons, protons, deuterons and tritons emerged from the target were stored at each angle corresponding to the experimental results.

5. RESULTS AND DISCUSSIONS

5.1 Neutron spectra

Fig. 1 shows the experimental and calculated neutron spectra. Neutron spectra measured in the forward direction have a plateau peak at high energy end which corresponds to about 60 to 70 % of the projectile energy per nucleon. This peak is mainly due to high energy neutron components produced in the forward direction by a break-up process and becomes more prominent for lighter target, since the momentum transfer from projectile to target nuclei are higher for lighter nucleus than for heavier nucleus. The high energy neutrons in the forward direction spread up to the energy which is about the twice as much as the incident particle energy per nucleon. The calculated spectra shown in Fig. 1 generally give rather good agreement with the experimental results in absolute values. Precisely speaking, the following three tendencies can be seen between experiments and calculations. In the calculation, a broad high energy peak in the forward direction appears more distinctly around incident particle energy per nucleon, compared with more flattened high energy peak in the experiment. This discrepancy also reveals that the LCS calculation gives the underestimation of the neutron spectra in the intermediate energy region of 5 to 50 MeV. The calculated spectra at angles larger than 30 degree are harder than the measured spectra, which means that the LCS calculation gives the underestimation of evaporation neutrons and the overestimation of pre-equilibrium neutrons extended to higher energy region.

5.2 Proton spectra

The experimental proton spectra are shown in Fig 2. The lower energy limit in the measured spectra was estimated to be 27MeV considering the proton energy absorption through the air between the target and the detector (500cm), the ΔE counter (0.5cm thick plastic of $CH_{1.104}$ and the density of $1.032 g/cm^3$) and the aluminum cover (0.5mm thick) of the E counter. These energy absorption was calculated for proton, deuteron and triton using the SPAR code [8], and the lower energy limits of proton, deuteron and triton which are reachable to the E counter are then estimated to be 27.0, 36.6 and 43.7MeV. Although proton spectra are similar to neutron spectra in shapes and absolute values at forward angles, proton yields rapidly decrease with increasing angles. At large angles, low energy proton components are dominant which can easily be absorbed by the thick target itself. Compared with measured and calculated proton spectra, the LCS calculation for proton spectra gives rather good agreement with the experiment in the forward direction.

5.3 Deuteron spectra

The experimental deuteron spectra are shown in Fig. 3. At 90 degree, the deuterons emitted from the target could not be detected because of its strong forwardness. Measured spectra in the forward direction have a broad peak around 140MeV and yields decrease drastically with increasing angles. For C target, the calculated and experimental results agree well at 0, 7.5, 15 and 60 degrees. At 30 degree, the calculated spectrum is larger than the measured one. As a general tendency, the agreement between calculated and measured deuteron spectra is surprisingly good.

5.4 Triton spectra

The experimental triton spectra are shown in Fig. 4. Triton could not be detected at 60 and 90 degrees because of much stronger forwardness than deuteron. Measured spectra in the forward direction have a broad peak around 200MeV and yields decrease drastically with increasing angles. In the triton spectra, the LCS calculation gives good agreement with the experiment in the forward direction, especially for heavier target.

6. CONCLUSION

We measured angular and energy distributions of neutrons, protons, deuterons and tritons produced by 100 MeV/nucleon helium ions stopping in carbon, aluminum, copper and lead targets. The experimental spectra were compared with the calculation using the LCS code and the calculated spectra are generally in rather good agreement with the measured spectra for these four secondary particles. These experimental results were found to be useful as the benchmark data for investigating the accuracy of high energy particle transport calculation code.

Acknowledgments

We gratefully acknowledge the support and assistance of the accelerator operation staff of HIMAC. This work was supported in part by the Research Project with Heavy Ions at NIRS-HIMAC.

References

[1] Cecil, R. A. et al., Phys. Rev., **C21**, 2471(1980)
[2] Heilbronn, L. et al., to be published in Nucl. Sci. Eng. May issue, 1999
[3] Kurosawa, T. et al., to be published in Nucl. Sci. Eng. May issue, 1999
[4] Kurosawa, T. et al., to be published in J. Nucl. Sci. Technol., January issue, 1999.
[5] Prael, R.E. and Lichtenstein, H., LA-UR-89-3014, Los Alamos National Laboratory (1989)
[6] Nakao, N. et al., Nucl. Instr. Meth. Phys. Res. **A362** 454(1995)
[7] Cecil, R. A. et al., Nucl. Instr. and Meth. **161** 439(1979)
[8] Armstrong T.W. and Chandler K.C., Oak Ridge National Laboratory Report ORNL-4869 (1973)

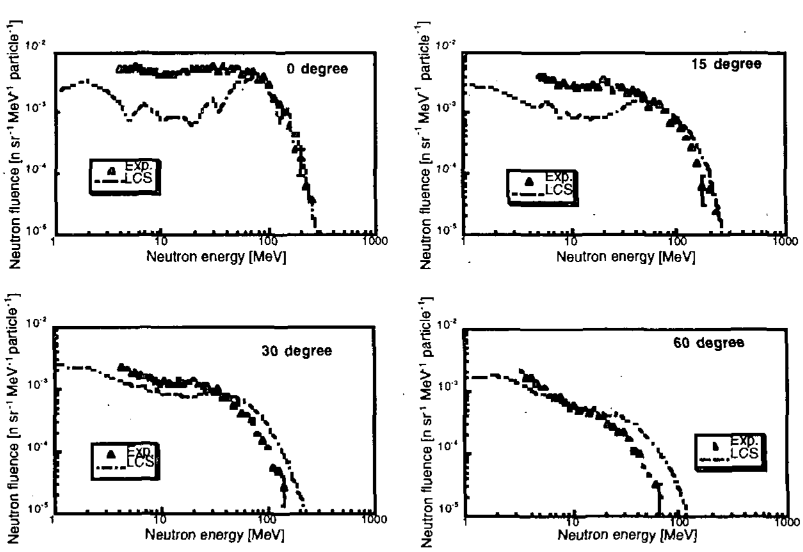

Fig. 1 Comparison of measured and calculated neutron spectra from carbon target.

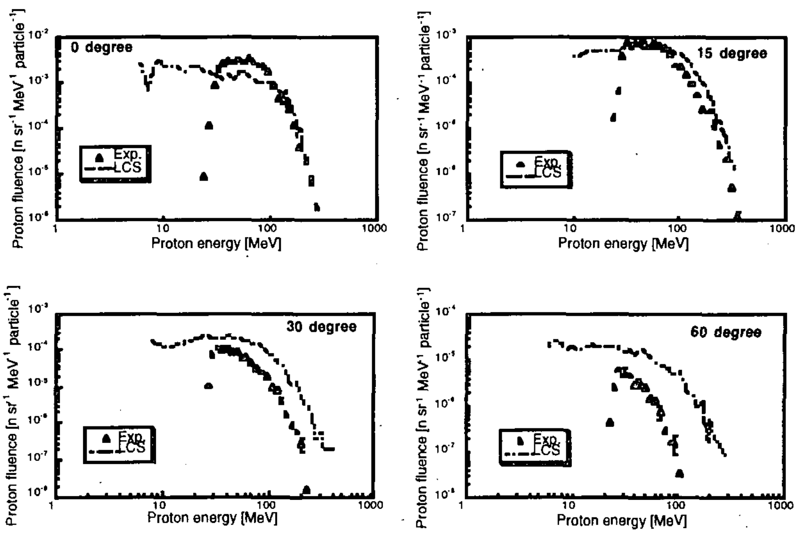

Fig. 2 Comparison of measured and calculated proton spectra from carbon target.

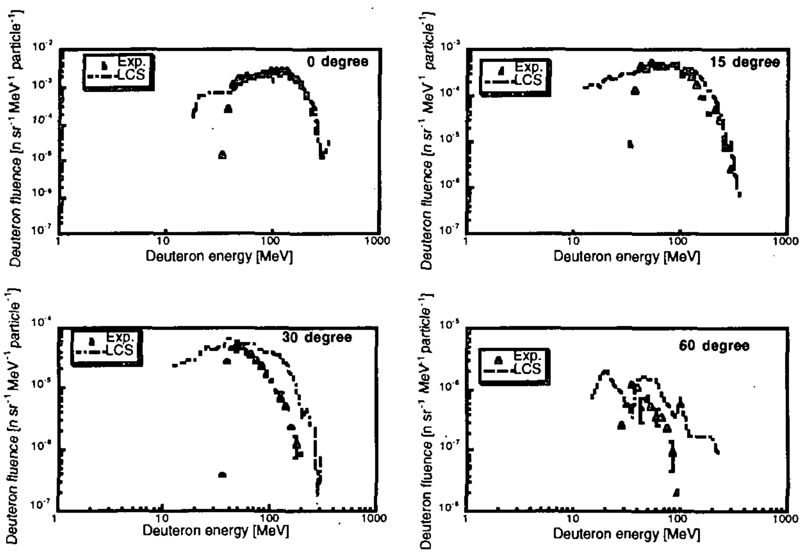

Fig. 3 Comparison of measured and calculated deuteron spectra from carbon target.

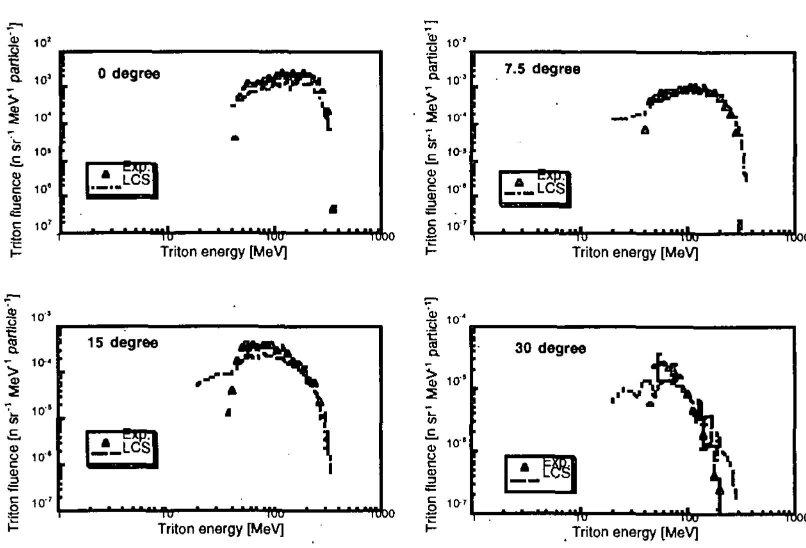

Fig. 4 Comparison of measured and calculated triton spectra from carbon target.

X. Tokyo Institute of Technology

X-1

Low-energy neutron direct capture by ^{12}C in a dispersive optical potential

H. Kitazawa, K. Go, and M. Igashira

A paper of this subject was published in Phys. Rev. C57, 202(1998), with the following abstract.

A dispersive optical potential for the interaction between low-energy neutrons and ^{12}C-nuclei is derived from a dispersion relation based on the Feshbach generalized optical model. The potential reproduces completely neutron total cross sections below 1.0 MeV, and substantially the energy of the 3090 keV($1/2^+$) level in ^{13}C which is of nearly pure $2s_{1/2}$ single-particle character. It is found that direct-capture model calculations with this potential explain quite successfully the observed off-resonance capture transitions to the ground($1/2^-$), 3090 keV($1/2^+$), 3685 keV($3/2^-$), and 3854 keV($5/2^+$) levels in ^{13}C at neutron energies of 20-600 keV. Special emphasis is laid on the fact that in those model analyses, account should be taken of the spatial nonlocality of the neutron-nucleus interaction potential, in particular for negative energies.

X-2

Nonresonant direct *p*- and *d*-wave neutron capture by ^{12}C

T. Kikuchi, Y. Nagai, T. S. Suzuki, T. Shima, T. Kii, M. Igashira, A. Mengoni, and T. Otsuka

A paper of this subject was published in Phys. Rev. C57, 2724(1998), with the following abstract.

Discrete γ rays from the neutron capture state of ^{13}C to its low-lying bound states have been measured using pulsed neutrons at E_n=550 keV. The partial capture cross sections have been determined to be 1.7±0.5, 24.2±1.0, 2.0±0.4, and 1.0±0.4 μb for the ground($J^\pi=1/2^-$) and first-($J^\pi=1/2^+$), second-($J^\pi=3/2^-$), and third-($J^\pi=5/2^+$) excited states, respectively. From a comparison with theoretical predictions based on the nonresonant direct radiative capture mechanism, we could determine the spectroscopic factor for the $J^\pi=1/2^+$ state to be

0.80 ± 0.04, free from neutron-nucleus interaction ambiguities in the continuum. In addition we have detected the contribution of the nonresonant *d*-wave capture component in the partial cross sections for transitions leading to the $J^{\pi}=1/2^{-}$ and $J^{\pi}=3/2^{-}$ states. While the *s*-wave capture dominates at $E_n \leqq 100$ keV, the *d*-wave component turns out to be very important at higher energies. From the present investigation the $^{12}C(n, \gamma)^{13}C$ reaction rate is obtained for temperatures in the range 10^7-10^{10}K.

X-3

Nuclear and nuclear astrophysical interest in $D(n, \gamma)^3H$ reaction

Y. Nagai, T. Kobayashi, T. Kikuchi, F. Okazaki, K. Takaoka, S. Naito, A. Tomyo, T. Shima, M. Igashira, and S. Ishikawa

A paper of this subject was published in Nuclear Instruments and Methods in Physics Research A 402, 408(1998), with the following abstract.

A neutron capture cross section of deuterium was measured for the first time at the neutron energies between 10 and 80 keV by detecting the prompt γ-ray from the capture state to the ground state of triton. The cross section is important to study the nuclear dynamics of the few nucleon systems, and to estimate the elemental abundances in the primordial nucleosynthesis. In order to pick up the small γ-ray signal from huge background we have developed highly sensitive NaI(TI) detector systems with good signal to noise ratio. Use of these detectors together with pulsed neutron beams enabled us to determine the small capture cross section accurately. The cross sections were obtained as 2.12(35) and 2.04(3) μ barns at 30.5 and 54.2keV, respectively, and they are compared with the theoretical ones.